NARSIS

New Approach to Reactor Safety ImprovementS

WP3: Integration and safety analysis

Del 3.3: Methodologies to constrain uncertainties in the components' modelling (causes and consequences)

This project has received funding from the Euratom research and training programme 2014-2018 under Grant Agreement No. 755439.

Project Acronym:	NARSIS		
Project Title:	New Approach to Reactor Safety Improvements		
Deliverable:	Del3.3: Methodologies to constrain uncertainties in the components' modelling (causes and consequences)		
Month due:	M42	**Month delivered:**	M42
Leading Partner:	BRGM		
Version:	FINAL		

Authors: Jeremy ROHMER, Pierre GEHL (BRGM), Irmela ZENTNER (EDF), James DANIELL (KIT), Slawomir POTEMPSKI (NCBJ)

Deliverable Review:

- **Reviewer #1:** Varenya DUVVURU MOHAN (TU Delft) **Date:** 15/01/2021
- **Reviewer #2:** Andrej PROSEK (JSI) **Date:** 14/01/2021

Dissemination Level		
PU	Public	**X**
PP	Restricted to other programme participants (including the Commission Services)	
RE	Restricted to a group specified by the consortium (including the Commission Services)	
CO	Confidential, only for members of the consortium (including the Commission Services)	

Table of contents

List of Figures

List of Tables

List of Abbreviations

Acronym	Definition	Page
ANCOVA	Analysis of Covariance Decomposition	15-16
ANN	Artificial Neural Network	50-53
BBN	Bayesian Belief Network	9-67
BBR	Boosted Beta Regression	24-47
BEMUSE	Best-Estimate Methods—Uncertainty and Sensitivity Evaluation	19
CIAU	Code with capability of Internal Assessment of Uncertainty	19-21
CPM	Conditional Probability Model	22-47
CPT	Conditional Probability Table	22-47
CSAU	Code Scaling, Applicability and Uncertainty	17-21
DAG	Directed Acyclic Graph	47
DM	Damage Measure	49
EDG	Emergency Diesel Generators	39-44
EPRI	Electric Power Research Institute	50
FAST	Fourier amplitude sensitivity test	13-21
FEM	Finite Element Model	50
FFTBM-SM	Fast Fourier transform based method by signal mirroring	19
GAMLSS	Generalized additive models for location, scale and shape	26
GRS	Gesellschaft für Reaktor- und Anlagensicherheit	17
GSA	Global Sensitivity Analysis	12-67
HCLPF	High Confidence Low Probability Failure capacity	53
IM	Intensity Measure	40-53
K-K NPP	Kashiwazaki-Kariwa nuclear power plant	50-53
LVSG	Low-Voltage SwitchGear	50
MCMC	Markov Chain Monte Carlo	49
NPP	Nuclear Power Plant	9-67
OAT	One-factor-at-A-Time	10-47
PDF	Probability Density Functions	17
PGA	Peak Ground Acceleration	51-53
Q-Q	Quantile-Quantile	27-47
SA	Sensitivity Analysis	9-67
SBO	Station Blackout	9, 21
SI	Sensitivity Indices	12-21
SQUG	Seismic Qualification Utility Group	49-53
STR	structural damage	39-53
UMAE	Uncertainty Methodology Based on Accuracy Extrapolation	18-21
VARS	Variogram Analysis of Response Surfaces	12

1 Executive Summary

Deliverable D3.3 addresses the question of constraining the uncertainties in the components' modelling (causes and consequences). Both NARSIS WP1 and WP2 involve complex models for respectively characterizing the physical external threats and the vulnerability and integrity assessment of NPP system components. In practice, this imposes processing a large number of sources of uncertainty whether regarding parameter uncertainty or model uncertainty. Building upon the recent best practices for uncertainty assessment, special attention is paid to characterize uncertainty pervading these models by adapting or developing techniques for sensitivity analysis, denoted SA.

The present report first provides an overview of the existing techniques / methods in the field of nuclear safety analysis. This shows that sensitivity analysis is a crucial task of any nuclear safety analysis. Its use is not new and in the past, numerous techniques have been developed to address this question whether for a local or a global analysis. The current overview also shows that there is no "one-fits-all" SA technique: depending on the characteristics of the problem, different techniques may be proposed or new developments are needed. The choice of particular techniques is then guided by the objective of the sensitivity analysis (local, global), the type of variables as well as the problem of dependence between inputs. Regarding NARSIS specificities, we have identified two aspects that deserve new developments for constraining uncertainties:

(1) Since Bayesian Belief Networks (BBNs) are one pillar of NARSIS (see deliverable D3.2), the question of SA is specifically addressed. The most widely used approach is based on sensitivity functions for discrete BBNs, and on partial derivatives for continuous BBNs. Reasons are the intuitive interpretation of the results (thanks to the graphical presentation) and the simplicity of the implementation. Yet, these approaches only provide information on the local influence, in the sense that the parameters are varied "one-at-a-time". This means that it can only provide a restricted vision on sensitivity, because the exploration of the sensitivity remains limited to a few Conditional Probability Model parameters, while the domain of the other parameters is left mostly unexplored. In this context, a newly developed Boosted Beta Regression approach (Rohmer & Gehl, 2020) broadens the scope of existing BBN-SA methods by providing a larger vision (global) on the influence related to the parameters of the Conditional Probability Model. The approach has the advantage of being generic (it can be applied to any kind of BBN, i.e. discrete, Gaussian or hybrid), and robust to the number of parameters (that can rapidly increase, typically reaching several dozens, even for moderate number of BBN nodes).

(2) The question of components' fragility is specifically addressed by relying on the developments of an approach for uncertainty reduction in fragility assessments. These results are also useful support to the developments in WP2 dedicated to fragility assessment of main NPPs (Nuclear Power Plant) critical elements. We have proposed a methodology within the Bayesian setting (Wang et al., 2018b) by combining an Artificial Neural Network, an adaptive training algorithm and an amplification-factor-based construction of the likelihood function. By application to the Kashiwazaki-Kariwa Research Initiative for Seismic Margin Assessment (KARISMA) benchmark, we have shown that the proposed procedure allows to reduce epistemic uncertainties (i.e. related to the lack of knowledge also named the reducible part of uncertainty) in the fragility curves. The application of the methodology was restricted to a seismic risk analysis, but it should be underlined that the framework is flexible enough to be extended to other hazards (and associated fragility curves), in particular because of the versatility of the Bayesian setting. Second, the application takes advantage of the availability of the damage database but could easily be applied to any inspection data coming, for instance, from in site monitoring exercises. This could constitute a valuable basis for NARSIS WP5 for instance.

2 Introduction

The present report addresses the question of constraining the uncertainties in the components' modelling (causes and consequences). Both WP1 and WP2 involve complex models for respectively characterizing the physical external threats and the vulnerability and integrity assessment of NPP system components. In practice, this imposes processing a large number of sources of uncertainty whether regarding parameter uncertainty or model uncertainty.

As a representative example, the finite-element model of an anchored steam line and of a supporting structure under seismic solicitations (as investigated by Gehl et al., 2019 and in NARSIS deliverable D2.6) implies accounting for several tens of different sources of parametric uncertainties (not to mention uncertainties related to the model set-up).

Building upon the recent best practices for uncertainty assessment (de Rocquigny *et al.* 2008, in collaboration with the European Safety Reliability Data Association), a special attention will be paid to characterize uncertainty pervading these models by adapting or developing techniques for sensitivity analysis, denoted SA (Iooss & Lemaître, 2015).

The objective of the present report is threefold:

1. Deliverable D3.3 aims at providing an overview of the existing techniques / methods in the field of nuclear safety analysis (Sect. 3);

2. Since BBN is one pillar of NARSIS (see deliverable D3.2), the question of SA is specifically addressed by relying on a newly developed technique dedicated to this specific method (Sect. 4);

3. The question of components' fragility is specifically addressed by relying on the developments of an approach for uncertainty reduction in fragility assessments, described in Sect. 5. These results are also useful in supporting the developments in WP2 dedicated to fragility assessment of main NPPs critical elements.

In this manner, most influential sources of uncertainty should be identified and prioritization for reducing them can be done accordingly so that uncertainty on modelling results can be constrained before integration within the BBN developed in WP3.

Note that the present report describes the methodologies developed within NARSIS project regarding the afore-described objectives. A companion deliverable D3.11 entitled "Constraining the uncertainties in the components modelling (causes and consequences) – Application to Station Blackout event" aims at specifically identifying, classifying and analysing the main sources of uncertainties that affect the progression and consequences for the major event of Station Blackout (SBO): these specific results may be used for the development of the Bayesian Network model (Task 3.2 - Building and integrating a BBN).

3 Overview of existing methodologies for constraining uncertainty in nuclear safety analysis

The objective of Sect. 3 is to provide an overview of the main methods for performing sensitivity analysis (denoted SA) in nuclear safety analysis.

The main aim of SA is to study the variability of model output under the variation of model parameters, in order to find which parameters actually have the highest impact on the model results. From ideological and technical points of view, one can distinguish between local (Sect. 3.1) and global (Sect. 3.2) sensitivity analyses. SA is often mentioned in tandem with uncertainty analysis, which tries to answer the question on the uncertainty of the results produced by the model (see de Rocquigny et al., 2008). It is obvious, that in this respect, the knowledge about the most sensitive model parameters plays a crucial role in analyzing propagation of uncertainties: Sect. 3.3 provides further details on the practices of uncertainty and sensitivity analysis for nuclear safety analysis.

3.1 Local SA

In the first SA approach, the idea is to investigate the model output by changing one factor at a time and fixing the rest to nominal values. This is the simplest and quite commonly used method known as on-at-a-time or one-factor-at-a-time (OAT) approach, and relies on some kind of perturbation scheme. On the other hand, the second approach is global in nature: model output is investigated over the entire range of input parameter values. Whichever approach is applied there is always a question about the sensitivity measure. The answer, however, very much depends on the used method.

In the case of local SA, in general, three main approaches can be discussed: derivative based methods, regression approximation and adjoint based analysis. Assuming the model output Y (in general it can be a vector) depends on the set of input parameters $X=(X_1, X_2,\ldots,X_n)$, one can investigate the magnitude of a partial derivative $|\frac{\partial Y}{\partial X_i}|$ at some fixed point in output space (explaining why the method is called local). The idea of using derivatives – as one can suspect – comes from the Taylor expansion of the quantity of interest Y, as it can predict which parameter has the highest impact on small perturbations of the input (which corresponds to the linear terms in the Taylor expansion).

In order to better compare derivatives of different parameters the scaled values are often used: either $\overline{X_k}\frac{\partial Y}{\partial X_k}$ or $\sigma_k\frac{\partial Y}{\partial X_k}$ i.e. scaled either by nominal parameter value or standard deviation of the considered parameter. In the first case it is called the scaled sensitivity parameter, while in the second case this is the sensitivity index (McClarren 2018). It is interesting, that with partial derivatives one can estimate the variance of Y using the following formula (^{T} denotes transposition):

$$Var(Y) \approx \frac{\partial Y^T}{\partial X}\sum\frac{\partial Y}{\partial X_i}. \qquad \text{(Eq. 1)}$$

It should be kept in mind that this is only the estimation of the variance, as no interaction between different parameters is taken into account. On the other hand, the estimation of partial derivatives can be easily obtained by the finite difference approximation (there are various formulas including high order approximations). There are also more sophisticated methods based on the solution of advection-diffusion-reaction differential equations, even with added stochastic terms – an example is shown in (McClarren 2018).

The idea that using the Taylor expansion can be extended to apply second order terms, means that second order derivatives have to be calculated. Then analogously, scaled sensitivity parameters can be calculated.

The second method used in local SA is based on regression approximation. Basically, it is also derived from the Taylor expansion. Consider $Y=(Y_1, Y_2,\ldots,Y_n)$ as quantities of interest and $X=(X_1, X_2,\ldots,X_n)$ as a set of parameters. Then using Taylor expansion one can get the following approximations:

$$Y(X_1) \approx Y(\bar{X}) + \nabla Y(\bar{X})(X_1 - \bar{X})$$

$$Y(X_2) \approx Y(\bar{X}) + \nabla Y(\bar{X})(X_2 - \bar{X})$$

……..…….

$$Y(X_n) \approx Y(\bar{X}) + \nabla Y(\bar{X})(X_n - \bar{X})$$

where $\bar{X}$ denotes nominal value. Then in order to find the vector $\nabla Y(\bar{X})$ after rearranging the above equations, one has to solve systems of linear equations of the form: $A\alpha=y$, where α is the vector of partial derivatives. As this system is not necessarily quadratic, typically the equation is multiplied by transposed matrix A^T leading to the equation $A^T A\alpha = A^T y$, which can be shown as equivalent to the least squares method i.e. the solution can be found as a minimization problem of the general form (here considering variable β):

α= {Find variable β such, that: $||A\beta-y||^2 \rightarrow \min$} (Eq. 2)

where appropriate norm ||·|| is selected.

However, this approach has a serious drawback, as the minimization problem can have a number of solutions in cases where the number of degrees of freedom is higher than the number of unknowns. Therefore, some regularization techniques are needed and applied.

Before the application of the regularization techniques, all unknowns are first normalized i.e. scaled values become the quantities to be found. Then some regularization method is used – the most popular are: Tikhonov, also known as ridge regularization (additional term of the form $\lambda||\beta||^2$ is added to minimized function), Lasso regularization (similar to Tikhonov but different norm is used in added term), and elastic net regression (where the added term is a combination of terms used in Tikhonov and Lasso regularizations). In any case, the regularization parameter λ (or two in elastic net regression) for ridge approach has to be selected. This is obtained by the so-called cross-validation approach, in which the whole data set is divided in two groups: training and test sets. This is repeated several times by random choice of the groups, and after the calculations with different parameter values, the set of errors are outputted. Then this set is treated statistically to find such parameter values which produce the smallest mean squared error (expressed usually by the standard deviation).

The regression approximation can be also utilized to find higher order terms in the Taylor expansion – again the unknowns are first scaled, and then bigger set of equations is solved by one of the minimization techniques.

The method based on the calculation of partial derivatives (both OAT or regression) is widely used in deterministic reactor safety analysis i.e.: neutronics and thermo-hydraulics (for example: Ronen 1986; Radulescu et al., 2008; Hernández-Solís 2012; Rearden 2000; Glaeser 2008; Strydom & Bostelman 2017, Qiu et al. 2016), and to some extent also in probabilistic risk analysis [Parkinson, Rasmussen, Hinkle 1979].

The other method for local SA is known as adjoint based analysis. Ideologically, the adjoint model in physics describes a reversed phenomenon. This is why it can be applied for generating information about perturbed quantities of interest – it describes how important some region in output space is for a particular quantity of interest. Probably the most attractive feature of adjoint SA is the fact that it can produce such information by solving only once original model without the need of solving it for perturbed parameters. This is obtained by solving both primary and dual models (for example, forward and backward). This means that by combining output from both models one can obtain sensitivity information about all parameters. Mathematically the adjoint operator is described by using inner product: $(Lu,u^*)=(u,L^*u^*)$, where L denotes original and L^* adjoint operator. Then two equations have to be solved $Lu = y$ and $L^*u^* = z$.

It can be easily checked that $(y, u^*) = (u, z)$. The quantity of interest can be often expressed as (u, z), hence, it can be calculated as (u^*, y).

Such an approach can be then applied to advection-diffusion-reaction type of differential equation (similarly as in one of OATs approaches). An example is given in Humbird & McClaren (2017), where the following advection-diffusion-reaction differential equation is considered:

$$v\frac{du}{dx} - \omega\frac{d^2v}{dx^2} + \tau(x)u = S(x) \quad \text{(Eq. 3)}$$

Where v, ω, τ correspond to, respectively advection, diffusion and reaction terms and S stands for the source. Some other similar examples can be found in Abdel-Khalik (2012), Cacuci (2015), Lemke et al. (2019).

This method looks attractive and elegant, but one should keep in mind that solving adjoint problems can also be computationally consuming. This is observed particularly in the case of non-linear or non-stationary problems, where some modifications of the described method must be introduced (for example Lagrange multipliers are often applied). Nevertheless, the adjoint based approach is applied to the problems in computational fluid dynamics, which need huge computational effort anyway (see for example Soto et al., 2004).

3.2 Local SA

As already mentioned, apart from local SA, the other approach is known as a global such as that used within NARSIS Deliverable 1.3 (Flood global sensitivity analysis). In this respect one can distinguish two main techniques: variance-based and variogram analysis of response surfaces (VARS).

In case of variance-based model the basic measure of sensitivity of each variable is the first-order Sobol index S_i (Sobol, 2001; Saltelli et al. 2019), which belongs to a big class of variance-based sensitivity measures and it is defined by:

$$S_i = \frac{V_i}{Var(OUT)}, \quad \text{(Eq. 4)}$$

where the numerator is defined as variance of conditional expectation of output (*OUT*) given input IN_i:

$$V_i = Var_{IN_i}\left(E_{IN_{\sim i}}(OUT|IN_i)\right). \quad \text{(Eq. 5)}$$

Thus, the first-order sensitivity index S_i measures the contribution to the output variance of the main effect of input variable IN_i, which is averaged over variations in remaining input parameters. The important feature of Sobol indices is the fact that they allow for global SA in which the impact of interactions between inputs on final output is accounted for. The formula above can be extended to investigation of the effect of two or more input variables in the following way:

$$S_{i_1 \dots i_n} := \frac{V_{i_1 \dots i_n}}{Var(OUT)}, \quad \text{(Eq. 6)}$$

where:

$$V_{i_1 \dots i_n} := Var_{IN_{i_1 \dots i_n}}\left(E_{IN_{\sim i_1 \dots i_n}}(OUT|IN_{i_1}, \dots, IN_{i_n})\right) - \sum_{k=1:n} V_{i_k} - \dots - \sum_{k=1:n} V_{i_1 \dots i_{k-1} i_{k+1} \dots i_n}.$$

Hence Sobol indices show the impact of the combination of different parameters on the output and thus non-linear effects are also taken into account (Homma & Saltelli, 1996). Technically, in order to make the calculations, methods based on Monte Carlo approach are typically used (for example regression correlation). In this respect there is always a question about optimization of simulations as they are time consuming. Other techniques, like Fourier amplitude sensitivity test (FAST) and various forms of differential analysis are also applied. For example in FAST coefficients from the multiple Fourier series expansion of the output function are used to represent conditional variances, and then transformation (based on some version of ergodic theorem) from multi-dimensional integral to a one-dimensional one is applied to find the Fourier coefficients. The problem of global SA is often related to screening process as it can help in decreasing the number of simulations required. Some modifications of Sobol indices are sometimes also proposed – for example using logarithmic values instead of original, as this better suits to linear regression technique.

An example of Sobol Indices in NARSIS D1.3 (Pheulpin & Bacchi, 2020; Pheulpin, 2020) for use in GSA (Global Sensitivity Analysis) in terms of variance-based methods is shown in Figure 1. It should be also noted that global SA can be applied in screening process in order to either eliminate non-sensitive parameters or vice versa to find the most sensitive ones for which normal OAT technique can be used. Some unified approach of this type has been proposed in Campolongo et al. (2011).

The VARS method is based on usage of variograms which, in principle, describe the degree of spatial dependence of the considered field. Variogram and covariograms are functions defined, respectively, by the following formulas:

$$\gamma(u - v) = \frac{1}{2} V[Y(u) - Y(v)] \quad \text{(Eq. 7)}$$

$$C(u - v) = \frac{1}{2} COV[Y(u), Y(v)] \quad \text{(Eq. 8)}$$

where *V* and *COV* are variance and covariance, *Y* represents output and *u*, *v* two points in space. The idea lies here in fact, that the usage of directional variograms and covariograms enables to identify the structures with spatial correlation of the output values *Y.* In consequence it allows also to estimate $|\frac{\partial Y}{\partial X_i}|$.

Recently a comparison between methods based on Sobol indices and variograms has appeared (Puy et al., 2020). The authors' conclusion is such that VARS method enriches the spectrum of various methods applied in SA and it rather complements than substitutes classic variance-based estimators.

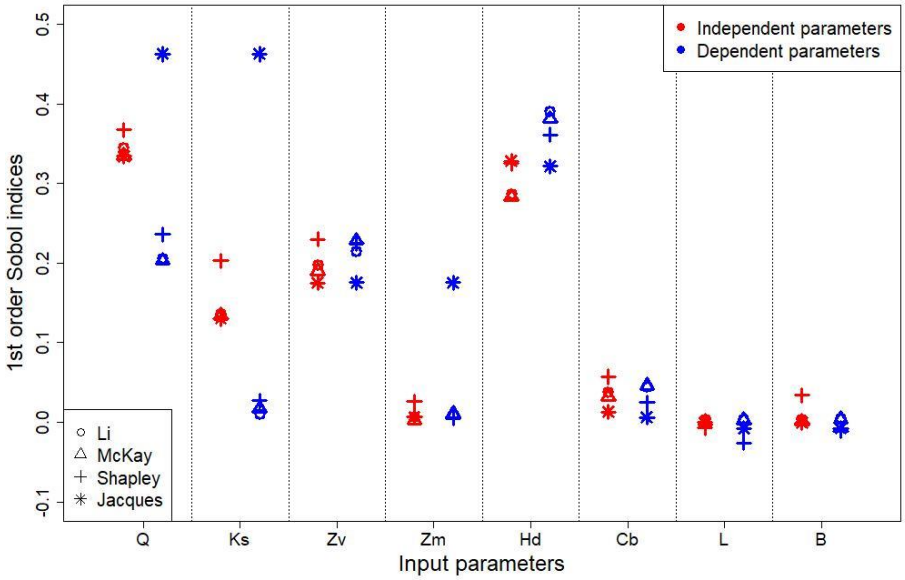

Inputs	Symbols	Units	PDF	Parameters
Maximal annual flow rate	Q	m^3/s	Truncated Gumbel	G(scale=1013, loc=558, min=500, max=3000)
Strickler coefficient	K_s	-	Truncated Normal	N(mean=30, sd=8, min=15, max=60)
River downstream level	Z_v	m	Triangle	T(min=49, mode=50, max=51)
River upstream level	Z_m	m	Triangle	T(min=54, mode=55, max=56)
Dike height	H_d	m	Uniform	U(min=7, max=9)
Bank level	C_b	m	Triangle	T(min=55, mode=55.5, max=56)
Length of the river stretch	L	m	Triangle	T(min=4990, mode=5000, max=5010)
River width	B	m	Triangle	T(min=295, mode=300, max=305)

Figure 1: Comparison between the first order SI calculated with four different methods (Li, McKay, Jacques and Shapley – see Table 1), and considering all the inputs to be independent or not (with the Jacques method, the SI are estimated for groups of dependent inputs) – extracted from Pheulpin & Bacchi, 2020; Pheulpin, 2020

In terms of performing GSA with dependent parameters, the following work in the hazards sphere is important to note such that some traditional methods of GSA initially designed for models with independent inputs have been adapted to models with dependent inputs. (Pheulpin & Bacchi, 2020; Pheulpin, 2020) identified more than 20 methods (reported in Table 1) to deal with dependent parameters. Most of them are variance-based methods allowing to compute sensitivity indices, useful to rank model inputs. For instance, some methods are based on a replicated Latin Hypercube Sampling (McKay, 1996), some others use an analysis of covariance (ANCOVA) decomposition technique. It allows to compute various sensitivity indices, as the uncorrelated contribution and the correlated one (Chastaing et al., 2012). The Shapley effects can also be computed with dependent inputs by using copulas (Iooss and Prieur, 2019). The last method (Table 1) is based on a screening technique. The classical screening Morris method, based on a discretization of the inputs in levels, has been adapted to models with dependent inputs by introducing copulas.

Table 1: Main methods to perform GSA with dependent parameters (SI means "Sensitivity Indices") after Pheulpin & Bacchi (2020) and Pheulpin (2020)

	Source	Computation of	Notes
1	Iman and Hora, 1990	Importance measure based on a metric distance between two distributions	
2	Chun et al., 2000		Improvement and extension of method n°**1**
3	Borgonovo et al., 2011	δ moment-free importance measure	
4	López-Benito and Bolado-Lavín, 2017		Application of the method n°**3** to a natural gas transmission model
5	Fang et al., 2004	SI estimated with a method based on sequential random sampling	Development of an algorithm based on multi-expressions of multinormal distribution to generate sequential random samples
6	McKay, 1995	Sobol' SI using LHS sampling	
7	Saltelli et al., 2004		
8	Ratto et al., 2004		
9	Oakley and O'Hagan, 2004	SI computed analytically through multidimensional integrals	Bayesian SA aiming to approximate the modelling function by a so-called "kriging" response surface
10	Jacques et al., 2006	Multidimensional SI	Extension of SI definition by taking into account blocks of correlations among the inputs
11	Da Veiga et al., 2009	SI based on local polynomial approximations for conditional moments	Intermediate method between n°**7** and n°**8**
12	Xu and Gertner, 2008	Various SI: Total contribution, uncorrelated contribution and correlated contribution	
13	Li et al., 2010		Extension of method n°**11**: ANCOVA decomposition technique (partial variance decomposed in a variance part and a covariance part) and use of High Dimensional Model Reduction (HDMR)
14	Pan et al., 2011		Application of the method n°**11** to a unsaturated flow and contaminant transport model
15	Li et al., 2011		Extension of method n°**11**: Decomposition of variance contribution of the correlated inputs based on the state dependent parameters
16	Mara and Tarantola, 2012		Alternative method of n°**12**: Decorrelation of the inputs with the Gram-Schmidt procedure and ANOVA-HDMR
17	Kucherenko et al., 2012		Alternative method of n°**12**: Computation of Sobol' SI based on Gaussian-copulas
18	Caniou, 2012		Extension of method n°**12**: Coupling of the ANCOVA technique with polynomial chaos expansion
19	Chastaing et al., 2012		Alternative method of n°**12** defining the SI using a Hoeffding-Sobol decomposition (inclusion of the covariance taking into account the dependency)
20	Zhou et al., 2013		Alternative method of n°**11** using a new algorithm avoiding the sampling procedure
21	Grandjacques et al., 2015	Sobol' SI for static and dynamic inputs	Use of Pick and Freeze sampling method
22	Li and Mahadevan, 2016	First-order Sobol' SI	Direct Sobol' SI estimation based only on input/output samples (model equations are not needed)
23	Iooss and Prieur, 2019	Shapley effects and Sobol' SI	SI computation allocates the mutual contribution (due to correlation and interaction) of a group of inputs to each individual input within the group
24	Wang et al., 2018c	Derivative-based SI using copula	Derivative-based sensitivity of variance contribution with respect to the distribution parameters. The dependence between inputs is described through copulas
25	Ţene et al., 2018	Elementary mean and standard deviation	Extension of the Morris' screening method allowing to take into account the dependencies between model parameters through copulas

3.3 Practices in nuclear safety: uncertainty and sensitivity analysis

The main application of SA in nuclear safety is strongly linked to uncertainty analysis. Therefore, it seems worth to mention such application, so the rest of this section will be devoted to a short review of the applied methods in this context.

Historically, one of the first methods to apply uncertainty assessment in complex systems analysis was CSAU (Code Scaling, Applicability and Uncertainty) developed by the U.S. Nuclear Regulatory Commission in late 1980s. This method was elaborated to systematically quantify uncertainties associated with simulations of nuclear reactors by taking into account data, physical models and nuclear power plant variability.

The CSAU methodology consists of three steps. The first one is aimed at identifying and ranking processes and phenomena which are important to the considered scenario being analysed. Thus, only the significant contributors to the overall uncertainty (the highly ranked phenomena) are selected to be evaluated.

In the second step, there are activities to assess the capability of the code to calculate processes important to the scenario by comparing calculations against experimental data to determine code accuracy as well as the scale-up capability, and to specify ranges of parameter variations needed for further studies (Zhao & Mousseau, 2012).

The last step involve the uncertainty analyses based on the response surface approach. In this method, the output is calculated as a function of selected input parameters of varying values when the rest of them are fixed (Figure 2). Thus, the higher the number of inputs considered the more cases must be calculated. Such an approach justifies the usage of a limited number of uncertain parameters in order to reduce the number of code runs and the cost of analysis (IAEA 2008).

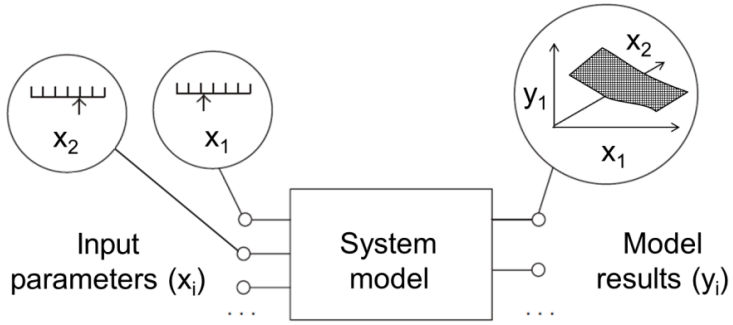

Figure 2: The system-output (yi) response surface as a function of input parameters (xi).

Despite of many successful applications, a lack of objectiveness and a high cost of CSAU have been criticized for the need of further improvement. The first one is related to the subjective judgement in ranking processes and phenomena to be evaluated in the context of uncertainty. This procedure heavily relies on expert opinions. The high cost is caused by need for large experimental database, many experts, and very high computational overhead.

Nevertheless, in different countries a number of uncertainty methods have been developed based on the CSAU principles. These methods, however, have progressed far beyond the CSAU approach and use more advanced techniques and procedures.

In the Gesellschaft für Reaktor- und Anlagensicherheit (GRS) method (the prototype of propagation of code input uncertainties) the state of knowledge about all uncertain parameters is described by the probability density functions (PDF) instead of simple ranging their values. Thus, in order to include information about uncertainties in the system-outputs, a number of code runs have to be performed. The input parameters that are fraught with uncertainties are sampled *n* times, and then the computer code generates *n* outputs which are used to estimate the actual uncertainty. However, for each of these calculation runs, all identified uncertain parameters are varied simultaneously (Figure 3).

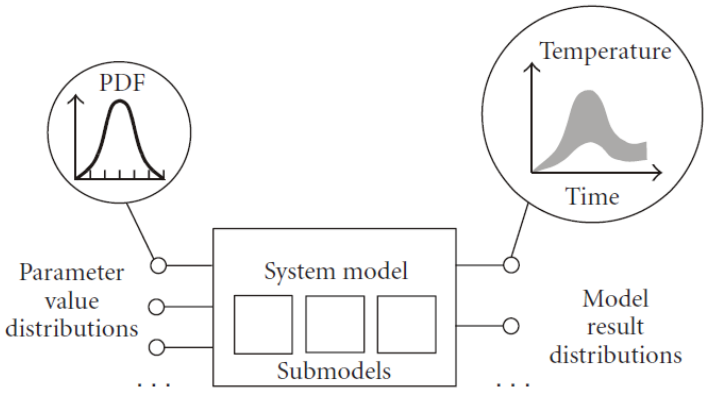

Figure 3: Consideration of probability distribution functions (PDF) in the GRS method (Glaeser 2008).

The advantage of using this technique is that the number of code calculations needed is independent of the number of uncertain parameters. The number of code calculations depends on the requested probability content and confidence level of the statistical tolerance limits used in the uncertainty statements of the results (Glaeser 2008). The required minimum number *n* of these calculation runs is given by Wilks' formula: $(1-\alpha/100)^n \geq \beta/100$, where *β* is the confidence level (%) that the maximum code result will not be exceeded with the probability *α* (%) given by the percentile of the corresponding output distribution, which is to be compared to the acceptance limit. For example, the 95th percentile value with a confidence level of 95% can be obtained for *n* = 59 when one-sided tolerance limit is considered.

This is a significant advantage of the GRS methodology when compared to the CSAU approach because no priori reduction in the number of uncertain parameters by expert judgment is necessary to limit the calculation effort. However, the challenge in performing uncertainty analysis with a usage of this methodology is the subjective specification of ranges and probability distributions of the input parameters (Frepoli & Petruzzi 2008).

In contrast to the GRS method the Uncertainty Methodology Based on Accuracy Extrapolation (UMAE) approach is focused not on the evaluation of individual parameter uncertainties but on calculation of the final uncertainty by comparing the simulation results with the experimental data. Thus, this is an example of a method based upon propagation of output uncertainties. The usage of this approach depends on the availability of experimental data for the specific system under investigation. In practice, however, it means it necessitates data from experiments performed for such a system but in a smaller scale (i.e. the integral test facility data).

For better representation of the real system the integral test facilities can be performed on a few different scales. The experimental data from such facilities are applicable to full scale system conditions, only if the test facilities the initial and the boundary conditions of experiments are properly scaled, for example, the scaling will not affect the evolution of physical processes important for the postulated accident scenario. This evaluation determines whether the data may be used in full scale system for a postulated accident scenario or not (Umminger & DelNevo 2012).

Assuming availability of the data and correctness of the code to simulate the experiments, it follows that the differences between code computations and the selected experimental data are due to the uncertainties. Then the resulting database is processed and the extrapolation to the full scale takes place. However, direct data extrapolation from small scale experiments to the full-scale system is difficult due to the imperfect scaling criteria adopted in the design of each scaled down facility. Thus, only the accuracy (i.e., the difference between measured and calculated quantities) is extrapolated (Petruzzi & D'Auria, 2008).

Since the deviations of code results from experimental data are quantified to evaluate the uncertainty of computer code models, the number of required code calculations is dependent on the number of integral experiments used to complete the comparison process (IAEA 2008).

While all uncertainty evaluation methods are highly affected by the resources needed for their application and the code-user dependence the new approach CIAU (Code with capability of Internal Assessment of Uncertainty) has been developed with the objective of reducing these limitations. The aim of the CIAU is to obtain uncertainty bands of the results that vary with time without additional input requirement nor special activity of the code user.

The idea of the CIAU approach is based on assumption that each status of the considered system can be described by a limited number of quantities (whose combination is called hypercube) and by the time instant when those values are reached. Then, the ranges of variation for those variables and the time are subdivided into intervals. Thus, each status of the system can be presented as a region of phase-space where the uncertainty in the code prediction is assumed to be uniform (Petruzzi & D'Auria 2008).

Assuming that the uncertainty for both quantities and time can be estimated to any status of the system by usage of the UMAE method one can implement the results back into the code. The code with implemented CIAU, available to the user in its final configuration, has the same features as the original code, and no additional input is needed to exploit the internal assessment of uncertainty capability.

This capability is implemented as an automatic post-processor where error bands are automatically generated and superimpose themselves on the calculated time trends. Therefore, no additional steps are required by the code user to run the original code if the CIAU is applied (IAEA 2008). This is the main advantage of this approach while the major limitation is still a necessity of the experimental data.

The BEMUSE (Best-Estimate Methods—Uncertainty and Sensitivity Evaluation) Programme – proposed by the Working Group on Accident Management and Analysis (WGAMA) of OECD/NEA and endorsed by the Committee on the Safety of Nuclear Installations (CSNI) – represents an important step towards the reliable application of high-quality best-estimate and uncertainty and sensitivity evaluation methods.

In phases 2 and 3 best-estimate and uncertainty and sensitivity evaluations of the thermal–hydraulic codes used for the calculation of the LOFT L2-5 test have been performed (de Crecy et al. 2008). All participants consider global sensitivities except the user of CIAU. In phase 4 and 5 best-estimate and uncertainty and sensitivity evaluations of a nuclear power plant have been performed (Perez et al. 2011). All participants using the probabilistic approach performed a sensitivity analysis. The computed influence coefficients were Pearson or value-based types, Spearman or rank-based types and variance-based type (Sobol indices).

In later study by (Prošek and Leskovar, 2015) it was shown that the proposed fast Fourier transform based tool by signal mirroring (FFTBM-SM) is complementary and a good alternative to the above mentioned typical statistical methods for sensitivity analysis. It can be used for comparing sensitivity runs performed by different participants. The results suggest that FFTBM-SM is especially appropriate for conducting quick analyses of judging impact of parameter variation in studies, in which several sensitivity calculations need to be compared or the influence of single sensitive parameters needs to be ranked. Namely, in BEMUSE, phase 2, there were 14 participants, each performing a reference calculation and up to 15 sensitivity runs of the L2-5 test carried out on LOFT facility.

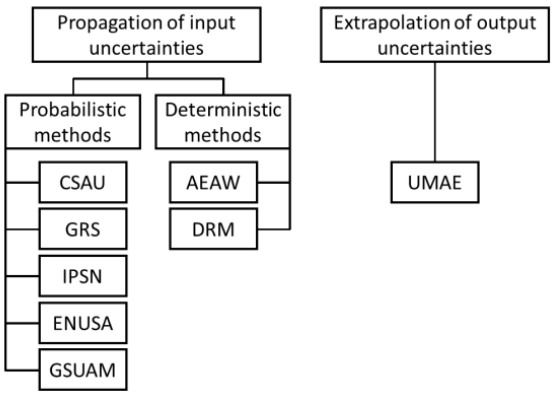

Figure 4: Uncertainty methods via Jaeger et al. (2017) – NUREG/IA-0462

As it can be easily seen, all the methods described, basically use a kind of SA that can be recognized as either local (CSAU, GRS) or global (UMAE, CIAU), for input uncertainties. For output uncertainties then UMAE is used, as seen in Figure 4, via the work in NUREG/IA-0462 by Jaeger et al. (2017).

There are also a number of uncertainty and SA codes as shown in **Erreur ! Source du renvoi introuvable.** incorporating components of the above analyses into them through (Skorek et al., 2019) and (Jaeger et al., 2017). These discuss the conservative approach versus best estimate plus uncertainties which have been discussed as part of NARSIS D3.9 and D3.10. A detailed application can also be found in D3.11, where uncertainties need to be quantified to ensure design is within acceptance criteria. Further details are provided by Prošek and Mavko (2007).

In addition, the reader is instructed to read de Rocquigny et al. (2008): Appendix B: a selection of tools and websites which has a few of those below and some additional tools for uncertainty and sensitivity analysis and more so within Marchand et al. (2018).

Commercial software packages such as Phimeca, STRUREL and Crystal Ball have not been included in the table.

Table 2: Main software tools for uncertainty analysis in nuclear power plants

Tool	Description
SUSA	Monte Carlo Program to quantify uncertainties of simulation codes, e.g. neutronic, thermal-hydraulic codes, etc. SUSA is developed by the Gesellschaft für Reaktor- und Anlagensicherheit (GRS). See https://www.grs.de/en/simulation-codes/susa
DAKOTA	Design Analysis Kit for Optimization and Terascale Application developed by Sandia National Laboratory (SNL). It is provided with a graphical user interface (SNAP) which is used for the input generation, manipulation and execution of TRACE simulations. See https://dakota.sandia.gov/download.html
OpenTURNS	Treatment of Uncertainties, Risks 'N Statistics was developed by EDF, EADS and Phimeca, trac.openturns.org/lib, and includes data analysis, probabilistic modelling, meta modelling but also reliability and sensitivity tools. See https://openturns.github.io/www/index.html
RAVEN	RAVEN is developed for multi-purpose uncertainty quantification, regression analysis, probabilistic risk assessment, data analysis and model optimization. It has been coupled to SAPHIRE previously. https://raven.inl.gov/SitePages/Overview.aspx, https://github.com/idaholab/raven
SUNSET	The SUNSET (Sensitivity and Uncertainty Statistical Evaluation Tool) software is a statistical tool providing a collection of methods for information treatment in risk analysis studies. Tool from IRSN (www.irsn.ir), coupled with an external code. It was also used in BEMUSE. See https://www.irsn.fr/EN/Research/Scientific-tools/Computer-codes/Pages/Sunset.aspx
URANIE	URANIE is developed by CEA (www.cea.fr) for sensitivity & uncertainty analysis and data assimilation and it is based on the ROOT framework (root.cern.ch) (CERN) (an object-oriented software multiplatform). It integrates a large amount of features enabled by Root and especially, C++ interpreter, SQL databases access, visualization tools and statistical analysis. See https://sourceforge.net/projects/uranie/
SIMLAB	A set of mathematical techniques for sensitivity & uncertainty analysis. See https://ec.europa.eu/jrc/en/samo/simlab
R	Many functions and packages for Uncertainty and Sensitivity Analysis such as "sensitivity", "CompModSA", "multisensi" etc. "Sensitivity" has global sensitivity analysis methods. There are a huge amount of other packages. See https://www.r-project.org/

3.4 Summary and implications for NARSIS

The afore-described state of the art shows that SA is a crucial task of any nuclear safety analysis. Its use is not new (Sect. 3.3) and in the past, numerous techniques have been developed to address this question whether for a local (Sect. 3.1) or a global (Sect. 3.2) analysis.

A detailed SA is provided in the companion deliverable D3.11 aiming at identifying, classifying and analysing the main sources of uncertainties that affect the progression and consequences for the major event of Station Blackout (SBO) by relying on a SA technique termed as fast Fourier transform based methods (Prošek et al., 2002).

The current overview also shows that there is no one-fits-all SA technique and depending on the characteristics of the problem, different techniques may be proposed or new developments are needed. The choice of the particular techniques is then guided by the objective of the SA (local, global), the type of variables as well as the problem of dependence between inputs (Table 1).

Regarding NARSIS specificities, we have identified two aspects that deserve new developments for constraining uncertainties:

1. for Bayesian Networks (NARSIS WP3): this is tackled in Sect. 4;
2. for fragility curves (NARSIS WP2): this is tackled in Sect. 5.

4 Sensitivity analysis in Bayesian Networks

Since BBN is one pillar of NARSIS (WP3 being dedicated to its development for nuclear safety analysis), the question of sensitivity analysis is specifically addressed here. Since available techniques show limitations regarding this objective (Sect. 4.1), we developed a new approach dedicated to this specific method (Rohmer and Gehl, 2020) that is tested on three application cases (Sect. 4.3 and 4.4).

4.1 Context and objectives

A Bayesian Belief Network (BBN) is widely recognized as a valuable modelling tool for expert systems (e.g. Russel et al., 2003). It has been applied in various complex domains, like ecosystems (Milns et al., 2010), genetics and biology (Scutari et al., 2014), industry (Weber et al., 2012), finance forecasting (Malagrino et al., 2018), marine safety (Hänninen et al., 2014), nuclear power plants (Kwag & Gupta 2017), coastal systems (Jäger et al., 2018), multi-hazard risk assessments (Gehl and D'Ayala, 2016), etc. An expert system has the ability to represent and reason on knowledge with the purpose of solving problems and giving advice (as defined by Jackson, 1999), by relying on three components (i.e. knowledge base, observation base, inference engine). Each of these components can benefit from the key features of BBN: (1) its capability to represent expert knowledge and to combine and integrate expert knowledge with information from any kind of sources, including experimental data, historical data, results from numerical simulations, etc.; (2) its high flexibility to model any causal relationships and to explicitly display the relationship among variables using a network-based approach, which can intuitively be understood by experts (Wiegerinck et al., 2010); and (3) its capability to answer probabilistic queries about them and to find out updated knowledge of the state of a subset of variables when other variables (the evidence variables) are observed. For instance, probabilistic queries in reliability assessments may correspond to finding the probability values of some failure cause given the observed damage level of the considered system. See Appendix A for a brief overview. The interested reader can also refer to Jensen (2001) for a complete introduction to BBN.

Formally, BBN is based on the graphical representation of the probabilistic relations among random variables by means of a directed acyclic graph composed of nodes (i.e. the states of the random variables) and arcs (i.e. dependency between nodes). See an example in Figure 6A. The nodes connected by an arc are called the parent and child nodes respectively. One child node may have several parent nodes, meaning that this node is affected by several factors. Similarly, a parent node could have several child nodes, meaning that this factor may have influences on several other factors. Conditional probabilities are the probabilities that reflect the degree of influence of the parent nodes on the child node. The probabilistic dependence (i.e. the relation cause-effect) is represented via a table called a Conditional Probability Table (CPT) when the variables X (nodes) are discrete. In this case, the CPT entries correspond to the probability value $\mathrm{P}(X_i = k|\,\mathrm{Pa}(X_i) = j)$ where k denotes the k^{th} possible level (either a discrete value or a category) that node X_i can take given that its parents $\mathrm{Pa}(X_i)$ take the j^{th} possible level. When the variables are continuous, the conditional distribution given its parents can typically be represented by means of a continuous probability distribution. The most popular model is the Gaussian distribution, as follows:

$$\mathrm{P}(X_i = y|\,\mathrm{Pa}(X_i) = \boldsymbol{x}) = G(y|m_0 + Z\boldsymbol{x}, S) \quad \text{(Eq. 9)}$$

where G is the Gaussian probability distribution whose mean is parameterized by a linear regression model with intercept m_0 and regression coefficients Z, and S is the conditional variance.

When the nodes are both discrete and continuous, different hybrid techniques exist in the literature (e.g., Murphy 1999; Shenoy, 2006; Beuzen et al., 2018).

Whatever the nature of the nodes, the pillar of any BBN-based results (either evidence propagation or inference) is the specification of the parameters of the conditional probability model (denoted CPM), i.e. the CPT entries or the regression coefficients of the linear Gaussian regression model. This process is recognized in the literature as one of the most delicate part of the BBN development (e.g., Chen & Pollino 2012; Druzdzel & van der Gaag 2000, etc.), which raises the question of confidence in the diagnosis or prognosis derived from the BBN-based expert systems (see discussion by Pitchforth & Mengersen, 2013). In the validation framework of BBN, SA tools play a major role in order to study how the output of a model varies with variation of the CPM parameters. Subsequently, the results from SA can be used as a basis for parameter tuning, as well as for studying the robustness of the model output to changes in the parameters (Coupé & van der Gaag 2002; Laskey et al. 1995).

For discrete BBNs, a widespread SA method relies on the use of sensitivity functions (Coupé & van der Gaag 2002; Castillo et al., 1997), which describe how the considered output probability varies as one CPT

entry value is changed. Some recent extensions have been proposed to conduct multi-way SA like the framework by Leonelli et al. (2017), i.e. SA when several CPT entries are allowed to vary. Effects of parameter changes can be described by the Chan–Darwiche (CD) distances (Chan–Darwiche 2002; 2005). The CD distance is used to quantify global changes by measuring how the overall distribution behaves when one (or more) parameter is varied. Likewise, SA approaches have been developed for continuous BBNs (mostly based on linear Gaussian regression) either based on computing partial derivatives (Castillo & Kjærulff 2003) or based on the use of divergence measures (Gómez-Villegas et al., 2007), with generalisation to multi-way SA (Gómez-Villegas et al., 2013).

Yet, several limitations of the existing SA methods exist.

(1) The SA methods differ depending on the type of BBN (discrete, continuous, hybrid);

(2) Though simple and efficient to implement, the approach based on sensitivity functions (combined with CD-distance analysis) remains local, because the values of only one parameter of the CPM is varied, while the other ones are kept constant. Multi-way SA methods have been proposed, but can rapidly become intractable. The SA procedure for Gaussian BBN presents the same limitation as being based on partial derivatives;

(3) The SA is usually performed by focusing on one type of co-variation of the different parameters (like proportional, uniform and order-preserving co-variation, see e.g., Renooij, 2014).

In the present study, we propose an alternative approach for SA, whose characteristics should complement the existing ones and overcome the afore-described limitations. The proposed approach should be:

- Global: since the sensitivity of any BBN-based probability of interest is affected by multiple variations in the CPM parameters, the sensitivity is studied in a global manner and the different parameters are allowed to be varied all together;
- Generic: it should apply to any kind of BBN, i.e. discrete, Gaussian or hybrid, with limited restriction on the type of variations of the CPM parameters;
- Robust to the number of parameters: the number of parameters can rapidly increase (in relation with number of nodes), typically reaching several dozens even for a moderate number of BBN nodes, which can hamper the interpretation of any global SA;
- Concise: the presentation of the SA results should be as intuitive as the sensitivity function method by using a graph-based approach.

To do so, we address the problem of SA for BBN with the viewpoint of regression by considering the BBN-based probabilistic queries P as the predictand and the CPM parameters as the predictors (denoted $\boldsymbol{C}$). In contrast to the classical regression model, which restricts the analysis to the expected value of P as a function of $\boldsymbol{C}$, we aim at estimating the full probabilistic variation of P by taking advantages of recent developments for distributional regression (e.g., Koenker et al., 2013). In the subsequent sections, we first describe the principles of the proposed method together with the implementation details (Sect. 4.2). In Sect. 4.3, we apply the approach to a small discrete BBN (6 nodes) used to capture medical knowledge (adapted from Cooper 1984) to exemplify the potentialities of the proposed approach. Then, in Sect. 4.4, two real cases are used to investigate the applicability of the proposed approach. Finally, Sect. 5 discusses the strengths and weaknesses of the proposed approach from the methodological and operational viewpoints.

4.2 Statistical methods

In this section, we first describe the principles underlying the development of the proposed approach (Sect. 4.2.1). We then provide the justifications for using Beta regression (Sect. 4.2.2) for sensitivity analysis of BBNs. Sect. 4.2.3 gives further technical details on the key ingredient of the procedure, namely the Boosted Beta Regression (BBR) technique. Finally, we describe how to check the adequacy of the BBR model to fit the data (Sect. 4.2.4).

4.2.1 Overall procedure

The different steps of the procedure hold as follows:

- Step1: generate perturbations of network's entry values ***C*** (i.e. the predictors) using, for instance, some random sampling techniques. For binary nodes, the CPT entries can be randomly perturbed using truncated Gaussian distributions (van der Gaag et al., 2013) ; for multi-level discrete nodes, it can be based on Dirichlet distributions (e.g., Young et al., 2009); for continuous Gaussian nodes, truncated Gaussian distributions can also be used if the purpose is to study the robustness to small-to-moderate variations; see also Gómez-Villegas et al. (2013) for alternative possible probability laws;
- Step 2: estimate the query probability of interest *P* derived from the inferences using the BBN. This probability value is the predictand;
- Step 3: establish the link between ***C*** and *P* using a regression model. We propose to rely on Beta regression models (see Sect. 4.2.3) using boosting-based fitting procedure (Sect. 4.2.2) to deal with the potentially large number of predictors;
- Step 4: check the adequacy of the Beta model by checking that the residuals are well approximated by the standard normal distribution (see Sect. 4.2.4).

4.2.2 Statistical methods

We choose to rely on the Beta regression model (e.g., Ferrari and Cribari-Neto, 2004) due to different difficulties inherent to our case. The first difficulty is related to the nature of the predictand, which lies within the interval [0, 1]. This prevents from a direct application of ordinary least squares (linear) regression techniques, because bounded data (such as rates and proportions- or here probability values) are typically heteroskedastic (e.g., Cribari-Neto and Zeileis, 2010), which means that their variance depends on the predictors' values.

Second, the distributions of such data are typically asymmetric, and the normal assumption underlying standard regression models might not be valid in our case. An alternative approach is to use regression models that are based on a probability distribution suitable for handling bounded data. A good candidate is the Beta law, whose density distribution *d* is defined as follows:

$$d(P,a,b) = \frac{\Gamma(a+b)}{\Gamma(a)\Gamma(b)} P^{a-1}(1-P)^{b-1} \quad \text{(Eq. 10)}$$

where Γ is the gamma function, (*a*,*b*) are the shape parameters. In the following, we preferably use an alternative parametrisation (μ,σ), where $\mu = \frac{a}{a+b}$ is the mean of *P* and $\sigma = \frac{1}{(a+b+1)^{1/2}}$ is related to the variance of *P,* i.e. $\mu(1-\mu)\sigma^2$ (e.g., Schmid et al., 2013) The σ-parameter allows covering a large spectrum of density shapes as shown in Figure 5 given different μ and σ values.

An additional difficulty is the inclusion of the boundary values at 0 and 1, because the density *d* in Eq. 11 is not defined at these values. This can be overcome by means of a simple transformation of *P* (Smithson and Verkuilen, 2006) as follows:

$$(P(n-1)+0.5)/n \quad \text{(Eq. 11)}$$

where *n* is the number of samples (i.e. the number perturbations performed to study the sensitivity of *P*).

The joint analysis of both Beta parameters (μ,σ) enables the BBN practitioners to investigate the sensitivity of the BBN with respect to two levels. The first level is related to the evolution of μ as a function of the CPM parameters. These evolutions can be interpreted in a similar manner as the sensitivity functions used in the traditional SA for BBN, but it is worth noting that these functions are global; in the sense that they are constructed based on samples where all CPM parameters are allowed to vary all together.

In the present study, we propose to introduce a second level of analysis by allowing the Beta σ parameter to vary as well. This is justified as follows:

- when the Beta σ parameter is incorrectly taken to be constant, some efficiency loss in the fitting process has been reported in the literature (e.g., Bayer and Cribari-Neto, 2017 and references therein);
- a potentially large number of predictors have to be handled in the regression model and we propose to select only one part of the CPM parameters that have influence on the BBN probabilistic query *P* (see Sect. 4.2.3). This means that for fixed values of these selected parameters, values of *P* can still vary due to perturbations of the CPM parameters that were left out. The σ parameter is here used to describe this type of variability;
- some algorithms for the estimation of BBN probabilistic queries are based on random sampling (like particle filter using logic sampling by Koller and Friedman (2009)), which may introduce some noise in the *P* estimates;
- studying the evolution of σ enables the BBN practitioners to identify the sources of data variability (e.g., Smyth and Verbyla, 1999) i.e. to study the influence on the uncertainty of *P*. In this manner, the BBN practitioners can identify different probabilistic regimes; e.g. situations where the probability of interest might switch from low to high values, i.e. situations of low to high risk. Such situations can be highlighted by low and high values of μ. Values of σ are then useful to indicate the confidence in the occurrence of such situations. For instance, high value of μ (high average value of *P*) together with low value of σ (low variance) provide strong evidence that changes in the considered parameter(s) might surely lead to situations of high probability. High values for both Beta parameters show, however, that the situation of high probability might occur but only with low confidence (i.e. high uncertainty).

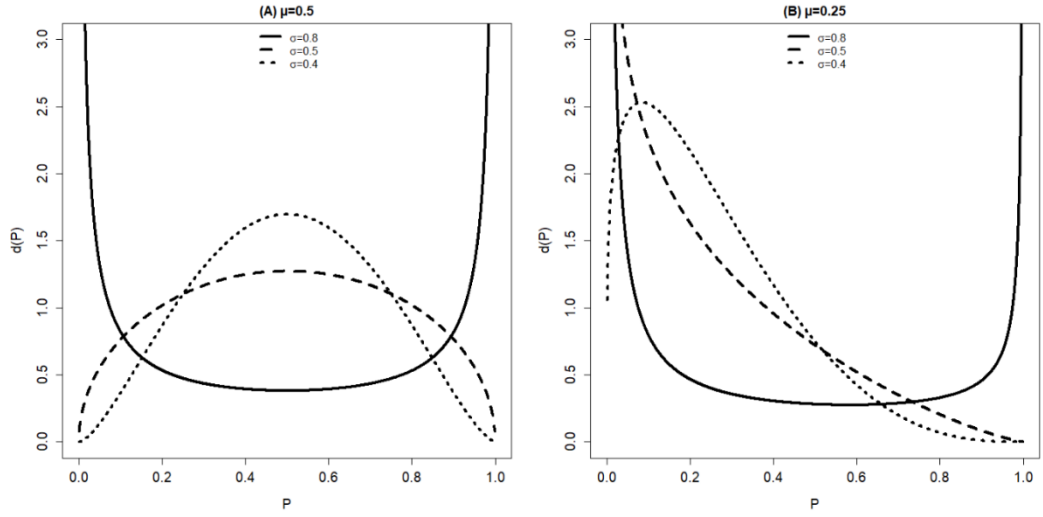

Figure 5: Probability density functions for the beta law. (A) mean μ=0.5; (B) mean μ=0.25.

Given the transformation of *P* (Eq. 11), BBN sensitivity analysis can be performed using Beta regression models (step 3 of the procedure) whose parameters are fitted using, for instance, maximum likelihood techniques (Cribari-Neto and Zeileis, 2010). Yet, the functional form of the predictor-predictand relationship (e.g., quadratic or exponential) can hardly be specified in advance in our case (except for specific cases, like binary discrete BBN) and the relationships should preferably be learnt from the data. A possible option can rely on more advanced Beta distribution regression techniques, for instance using generalized additive models for location, scale and shape (GAMLSS, Rigby and Stasinopoulos, 2005), which allows deriving smooth non-linear functional terms from the data, which correspond to the "partial effects" (more formally introduced in Sect. 4.2.3). These terms are the key ingredients for sensitivity analysis, because they hold the information of each parameter's individual effect on the considered Beta parameter.

The difficulty in our case is, however, the possible large number of predictors, which can typically exceed several tens in real cases. This situation imposes the use of techniques for variable selection during the fitting process. A possible option is the combination of GAMLSS with boosting-based approach (Mayr et al., 2012), which is detailed in the next section.

4.2.3 Boosted Beta Regression

In contrast to classical regression model, GAMLSS for Beta probability distribution aims at regressing the Beta parameters $\boldsymbol{\theta}=(\mu,\sigma)$ (or their transformation, e.g. via a log or a logit function) to the *p* predictor variables $\boldsymbol{C}=(c_1, c_2,\ldots, c_p)$, e.g., the CPT entries for discrete BBN or the regression coefficients of a Gaussian BBN. In the following, we restrict the analysis to a semi-parametric additive formulation as follows:

$$\theta = \eta_\theta(\boldsymbol{C}) = \beta_0 + \sum_{j=1}^{J} f_j(c_j|\beta_j) \quad \text{(Eq. 12)}$$

where $\eta_\theta(.)$ is the link function that relates the considered parameter $\boldsymbol{\theta}=(\mu,\sigma)$ with the predictor variables $\boldsymbol{C}$; $J \leq p$, β_0 is a constant and the functional term $f_j(.)$ corresponds to a univariate smooth non-linear model like penalized regression P-spline models (Eilers and Marx 1996) with parameters β_j. These functional terms (termed as partial effect) hold the information of each parameter's individual effect on the considered Beta parameter.

The fitting is performed using the *gamboostLSS* algorithm of Mayr et al. (2012), which uses the Beta log-likelihood function (termed as risk) as an optimization criterion based on the component-wise gradient boosting technique (Bühlmann and Hothorn 2007, see further details in Appendix B). The approach is termed as BBR model (Boosted Beta Regression).

One advantage of using boosting techniques is to perform variable selection during the fitting process, which allows screening the parameters $\boldsymbol{C}$ which hold most information with respect to the conditional distribution of *P*. This is performed by assessing the individual fits of each predictor variable, and by updating only the coefficient of the best-fitting predictor variable in each iteration. Variable selection is carried out successively for the mean μ and for the σ parameter.

When the algorithm is stopped, the final model only contains the set of best-fitting predictors. The number of boosting iterations controls the smoothness of the non-linear effects. Low values lead to sparse models with smooth functional terms, whereas large values lead to more complex models with larger number of predictors and rougher functional terms. In practice, the selection of the stopping parameter can be carried out using cross-validation procedures in order to optimize the risk on observations left out (i.e. "out-of-bag") from the fitting process i.e. the out-of-bag risk, which corresponds here to the negative log-likelihood of the Beta distribution calculated for the "out-of-bag" samples. To avoid optimizing two different stopping iterations, i.e. one for each Beta parameter, the procedure can be enhanced using the noncyclic algorithm of Thomas et al. (2018), which allows reducing the optimisation problem from a multi-dimensional to a one-dimensional problem.

In some situations, the resulting BBR model can still remain too rich to be easily interpretable by BBN practitioners. This procedure can be completed by the stability selection analysis (described in Appendix C), which allows screening the most influential variables in the BBR model.

In summary, the boosting-based approach allows to both select a limited number of influential predictors among all network's entry values $\boldsymbol{C}$, and to derive the corresponding partial effects for each Beta parameter. Note that the identified predictors are not necessarily the same for μ and for σ, and can be unique or multiple. The final results of the procedure are the partial effects (Eq. 12), which can directly be used to analyze the sensitivity of the considered Beta parameter to $\boldsymbol{C}$ as illustrated on the application cases (Sect. 4.3 and 4.4), by considering two levels of analysis (respectively related to the best estimate of *P* using μ, and to the uncertainty of *P* using σ).

4.2.4 Model adequacy

Once the BBR model has been fitted, an important aspect is to check the model adequacy (step 4 of the procedure), i.e. how well the BBR model is appropriate to describe the randomly generated BBN-derived probabilities. This can be done by analysing the statistics of the residuals and checking whether their distribution is well approximated by the standard normal distribution (see e.g. Rigby and Stasinopoulos, 2005). Yet, contrary to ordinary least square regression, the raw response residuals $r = P - \mu$ cannot be used, because they do not account for the heteroscedasticity of the model (i.e. the variance of *P* is a function of the Beta mean μ, see Sect. 4.2.1).

In the following, we propose to keep the analysis of *r* in order to give information regarding the capability of the Beta mean to explain *P*. However, to properly validate the use of the Beta model, we rely on alternative residuals' formulations (see e.g., Pereira, 2019 and references therein). We focus here on three of the most widely-used ones described in Appendix D. The normality of these residuals is

investigated by means of the normal Q-Q plot and by computing the coefficient of determination R^2 as follows:

$$R^2 = 1 - \frac{\sum_{k=1}^{k=N}(\widehat{q_k} - q_k)^2}{\sum_{k=1}^{k=N}(q_k - \bar{q})^2} \quad \text{(Eq. 13)}$$

where N is the number of quantile levels; q_i is the quantile of standard normal distribution at the kth level; $\bar{q}$ is the mean of the quantile of standard normal distribution over the levels k=1…N; $\widehat{q_k}$ is the quantile of BBR residual at the kth level. The closer R^2 to one, the better the agreement between the BBR residuals' quantiles and the ones of the standard normal distribution, hence the more satisfactory the adequacy of the BBR model. Furthermore, studying the evolution of R^2 as function of the number of random perturbations of $\boldsymbol{C}$ provides an option to estimate the minimum number of required permutations for the BBR model to be valid.

It should however be underlined that the residuals are analysed with the objective of checking that the Beta distribution is an appropriate model to explain the BBN-derived probabilities. Using them for another objective, for instance to compare different probability model families (e.g. Gamma, Gaussian) or to perform predictions, is made difficult by the use of boosting algorithms (see Hofner et al., 2016: Sect. 5.4). For these purposes, the use of the out-of-bag risk is recommended.

4.3 Synthetic case study

In this section, we consider a BBN of small number of nodes (described in Sect 4.3.1) to exemplify the functionalities of the proposed approach (Sect. 4.3.2).

4.3.1 Description

We focus on the BBN adapted by van der Gaag et al. (2013) from Cooper (1984) in the field of oncology. The network (as depicted in Figure 6A) is composed of 6 nodes and 6 arcs.

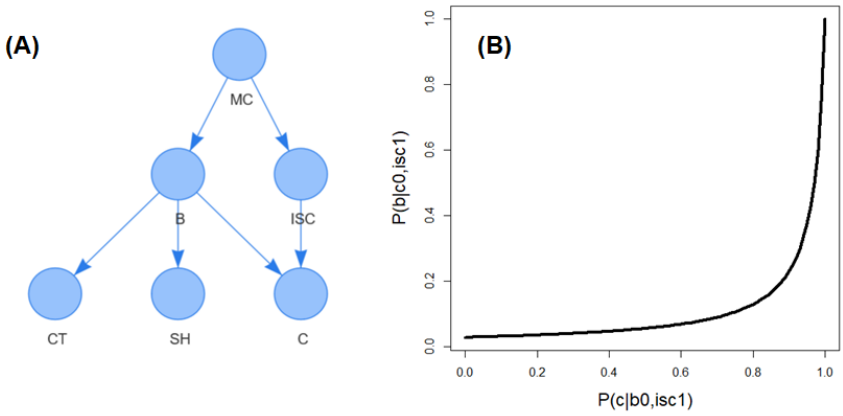

Figure 6: A) Brain tumor structure network; B) Sensitivity function derived by van der Gaag et al. (2013) showing the evolution of the probability of interest P(b|c0,isc1) as a function of the CPT entry P(c|b0,isc1).

Node MC refers to metastatic cancer, which may potentially lead to the development of a brain tumour (node B) and may give rise to an increased level of serum calcium (node ISC). The presence of a brain tumour can be established from a CT scan (CT). Another indicator of the presence of a brain tumour can be related to severe headaches (SH). A brain tumour or an increased level of serum calcium are both likely to cause a patient to fall into a coma (C). The conditional probabilistic relationships between the nodes (CPT entries) are provided in

Table 3. We focus here on the probability P=*P(b|c0,isc1), namely the probability to develop brain tumor given the absence of coma and an increased level of serum calcium. The robustness of* P *is studied with respect to the values of 13 CPT entries (*

Table 3).

Table 3: CPT entries for the brain tumor BBN. For instance P(c|b0,isc1) corresponds to the probability of node C being in state 1 conditioned by the fact that node B is in state 0 and ISC is in state 1. The meaning of the other probabilities should be understood following this example.

Node	Conditional probability
MC	P(mc)=0.20
B	P(b|mc1)=0.20 P(b|mc0)=0.05
ISC	P(isc|mc1)=0.80 P(isc|mc0)=0.20
C	P(c|b1)=0.95 P(c|b1,isc1)=0.80 P(c|b1,isc0)=0.80 P(c|b0,isc0)=0.05
CT	P(ct|b1)=0.95 P(ct|b0)=0.10
SH	P(sh|b1)=0.80 P(sh|b0)=0.60
MC	P(mc)=0.20

4.3.2 Application

We now apply the proposed BBR approach. It starts with the random sampling of the 13 CPT entry values using Gaussian distributions (with a standard deviation of 0.1 for all the 13 CPT values) truncated at zero and one as proposed by van der Gaag et al. (2013). For each of the randomly generated values of the CPT entries, the probability of interest *P*, i.e. P(b|c0,isc1), is calculated through approximate Bayesian inference based on particle filter using logic sampling (Koller and Friedman 2009). Note that other approaches for inference can be adopted especially when the *P* of low value (see e.g., Scutari et al., 2014). These values are then transformed using Eq. 11.

The minimum number of random perturbations of the BBN was chosen by studying the evolution of the R^2 indicator values for the different residuals' formulations (see Appendix D). Figure 7A shows that the convergence can be considered reached for a minimum number of ten times the number of CPT entries, i.e. 1,300 for which the R^2 values all reach very satisfactory values above 95%. The visual inspection of the normal Q-Q plots in Figure 7B-D confirms the satisfactory adequacy of the BBR model. We can however note some deviations for very low quantile values but this is only indicated by one residuals' formulation (Figure 7C). Besides, taking into account the 95% confidence band (outlined by dashed lines in Figure 7C), this discrepancy can be considered low.

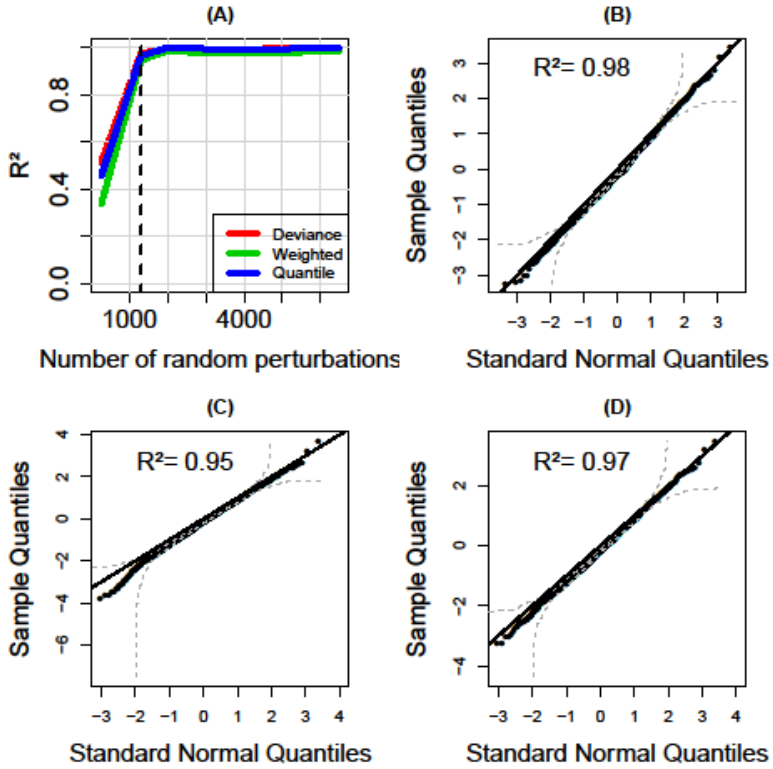

Figure 7: (A) Evolution of the R^2 indicator as a function of the number of random perturbations for the brain tumor BBN. Three residuals' formulations are considered (see Appendix D). The vertical dashed line indicates the selected number of random perturbations. For this number, normal Q-Q plots are provided considering different residuals: (B) deviance; (C) standardized weighted; (D) quantile. The dashed lines indicate the boundaries of the 95% confidence band based on the Kolmogorov-Smirnov statistic (Doksum and Sievers, 1976). The value of the R^2 indicator (Eq. 13) is also reported.

The histogram of the probability of interest *P* values is provided in Figure 8A with mean and standard deviation at respectively 0.18 and 0.14. Figure 8B shows that the Beta mean is informative regarding *P* and satisfactorily explains *P*, which is in agreement with the analysis of the Q-Q plots (Figure 7). Some deviations can however be noticed for very large values, but may be related to the low number of data to perform the fitting (see the light colour in Figure 8B indicating a low density of dots). The optimal stopping iteration of BBR model is selected by a 5-fold cross validation procedure (combined with the noncyclic algorithm of Thomas et al., 2018) as illustrated in Figure 8C.

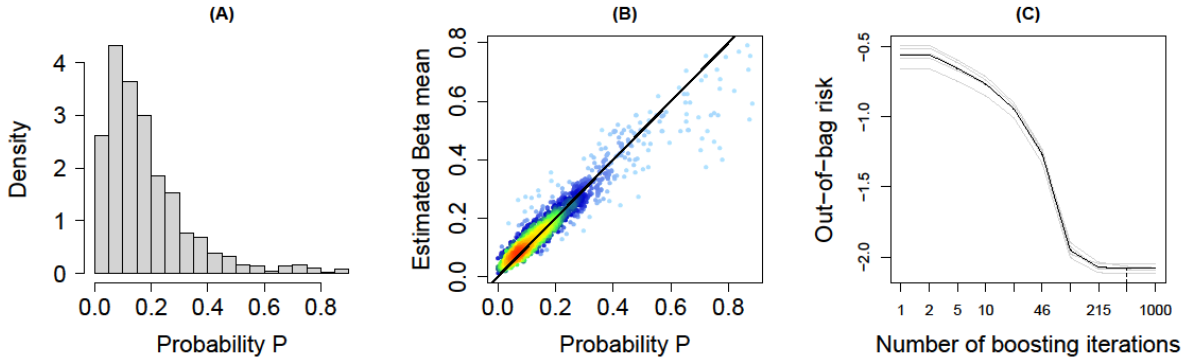

Figure 8: (A) Histogram of randomly generated P values for the brain tumor network; (B) Comparison between the estimated Beta mean and P (the colours indicate the density of the dots); (C) Evolution of the (out-of-bag) risk estimated using a 5-fold cross-validation procedure as a function of the number of boosting iterations; the optimal stopping iteration is selected as the one minimizing the average risk over all 5 cross-validation iterations (indicated by a vertical dashed line at 464).

Figure 9 and Figure 10 respectively depicts the non-linear effects on μ and σ of the CPT entries selected by the boosting algorithm during the fitting of the BBR model. Different conclusions regarding the sensitivity of *P* to the CPT entries can be drawn:

- Information on the importance ranking of the CPT entries can be derived. We show that only 7 out of the 13 CPT entries have been selected by the boosting algorithm, namely the CPT entries related to the nodes MC, ISC and C in direct relation with node B (see Figure 6A);
- The individual contributions of the selected CPT entries in Figure 9 and Figure 10 are global in the sense that they are constructed by accounting for the co-variations of all inputs (contrary to the traditional SA using sensitivity functions, which imposes the construction of the function by varying one input one at a time);
- Information on the type of effect the CPT entries can be derived. We show that the CPT entries' effect on the Beta mean μ is monotonic but rarely linear. In particular, the effect of P(c|b0,isc1) almost follows an exponential-like trend (outlined by dashed red lines in Figure 9, bottom right hard corner), which is in agreement with the traditional SA of *P* (Figure 6B) using a sensitivity function of polynomial form (as derived by van der Gaag et al. 2013);
- The effect on the Beta parameter σ is also nonlinear with respect to the selected CPT entries, hence indicating that the CPT entries not only affect the best estimate of *P* but also its precision, i.e. dispersion of the underlying Beta law.

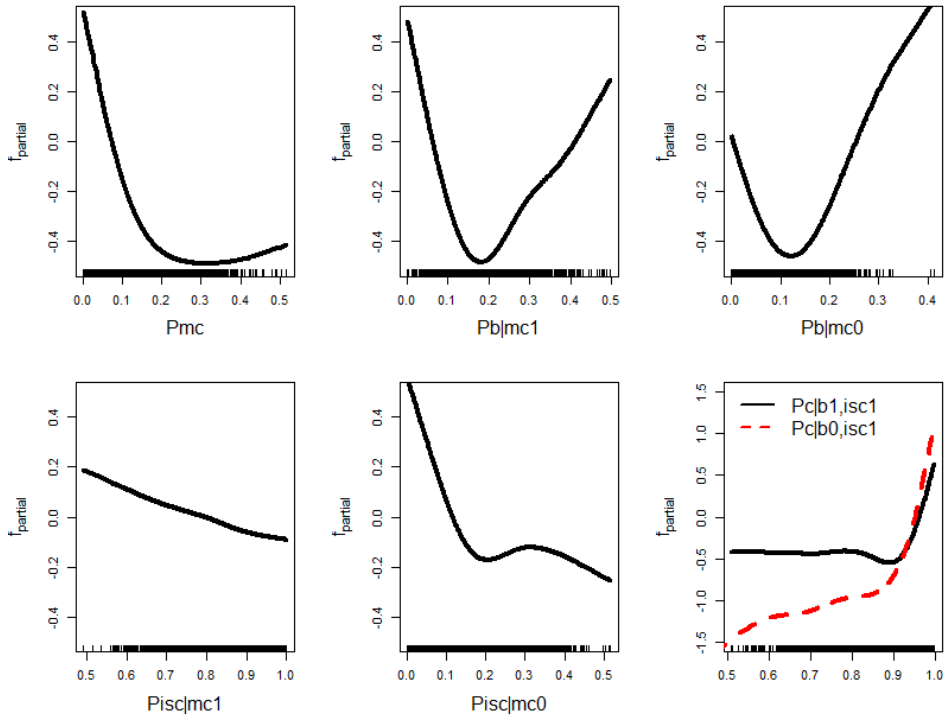

Figure 9: Partial effect of each CPT entry on μ (logit-transformed) applied to the brain tumor network. Note the different scales of the x- and y-axis.

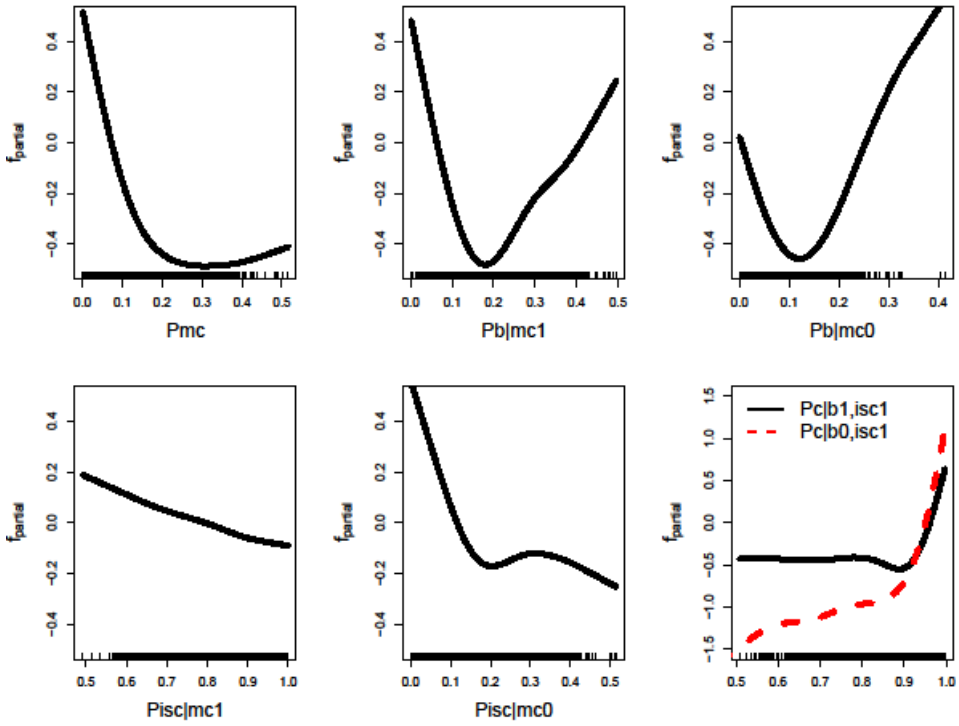

Figure 10: Partial effect of each CPT entry on σ(logit-transformed) applied to the brain tumor network. Note the different scales of the x- and y-axis.

Since the partial effects in Figure 9 and Figure 10 are global, these can easily be used by varying each CPT entries one-at-a-time or jointly.

Figure 11 (top) depicts the results of such analysis considering the individual variation of P(c|b1,isc1) and of P(c|b0,isc1) on the Beta density function related to P *(while keeping the other CPT entry values at their original values as provided in*

Table 3).

- When P(c|b0,isc1) is varied from low to high values (Figure 11A), the corresponding Beta density function is translated from low to high values, but with more and more dispersion around the mode, which is more specifically amplified when P(c|b0,isc1) exceeds value of ~0.9;
- When P(c|b1,isc1) is varied from low to high values (Figure 11B), the effect on the Beta mode is opposite to the one due to the effect of P(c|b0,isc1). This exemplifies the decreasing trend outlined in Figure 9 (bottom right hand corner): the mode is translated from high to low values with an effect on the dispersion less pronounced than for P(c|b0,isc1). This is in agreement with the lower partial effect outlined in Figure 10(bottom right hand corner);
- Finally, Figure 11C depicts the result of the analysis when both CPT entries are jointly varied. This shows that the impact of both CPT entries is compensated when they are jointly increased similarly: the Beta distributions remains “stuck” around 0.15 unless both CPT entries reach very high values above 0.95.

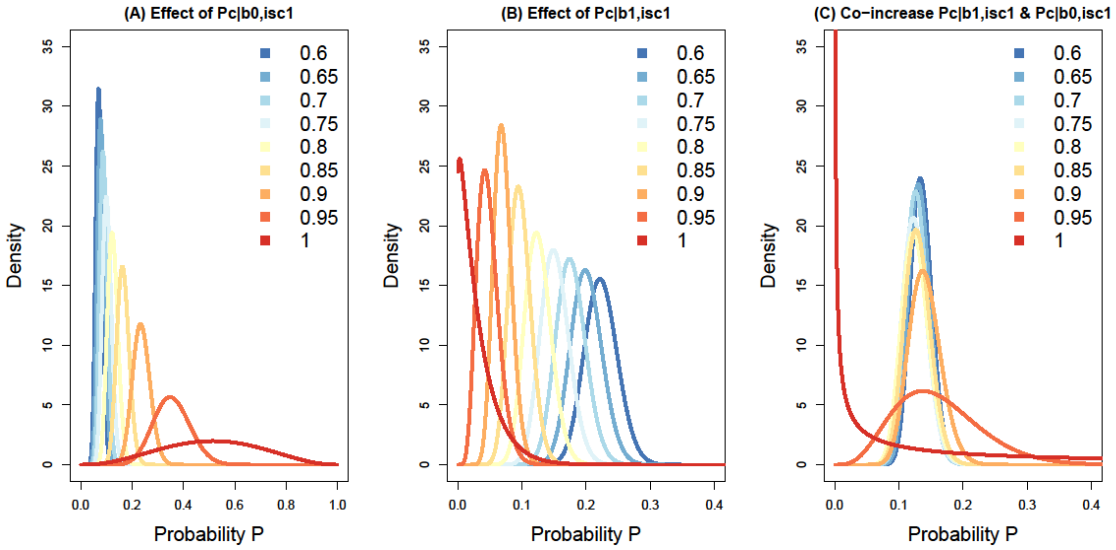

Figure 11: (A) Evolution of the Beta law fitted to the P values given increasing values of P(c|b0,isc1) from low (0.6) to high values (1.0); (B) Evolution of the Beta law fitted to the P values given increasing values of P(c|b1,isc1) from low (0.6) to high values (1.0); (C) Evolution of the Beta law fitted to the P values given increasing values (with same increment) of both P(c|b1,isc1) and P(c|b0,isc1).

4.4 Real-case applications

In this section, we apply the BBR approach to real cases. First, a linear Gaussian BBN is considered for assessing the damage of reinforced concrete structures (Castillo and Kjærulff, 2003). This enables us to illustrate a situation where the number of parameters is large enough to hamper the interpretation, i.e. here more than 40 variables have to be processed (Sect. 4.1). Second, a discrete BBN is considered for reliability analysis. For this case, analytical sensitivity functions can hardly be derived since the interest is not the sensitivity to the values of the CPT entries directly, but the physical parameters, which determine them.

4.4.1 Reinforced-Concrete BBN

We investigate the robustness of the BBN presented in Castillo and Kjærulff (2003) for assessing the damage of reinforced concrete structures (Figure 12).

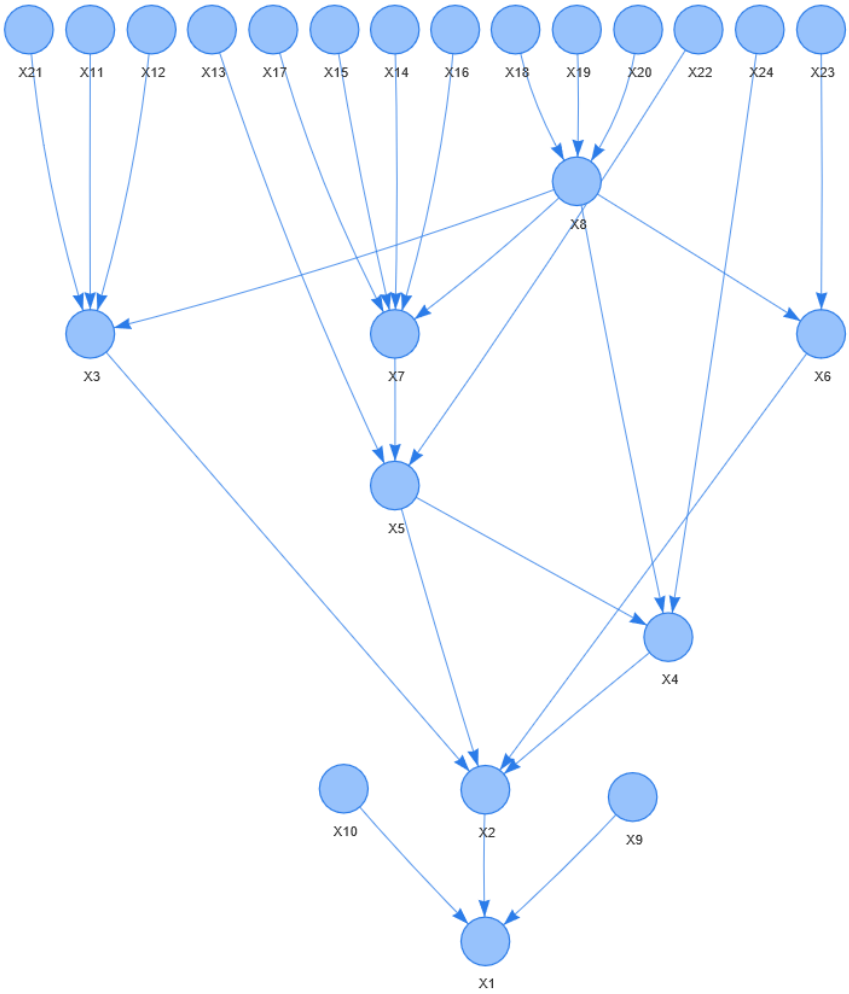

Figure 12: Structure of the reinforced concrete network.

The BBN is composed of 24 continuous nodes, 27 arcs and more than 40 parameters. The random variables (see nodes' meaning in

Table 4) are assumed to be normally distributed.

The original parametrization of Castillo and Kjærulff (2003) follows the regression model in Eq. 9 and assumes zero mean for all variables (i.e. nil intercept m_0), and conditional standard of 1.0 for observable nodes (i.e. X_9-X_{24}) and 10^{-4} otherwise (term denoted s_0 in Table 5). Values for the regression coefficients are provided inTable 5. In the following, we refer to these values as the CPM best estimate for the BBN parametrization.

We investigate the robustness of the probability for the damage of the system X1≥1 given the evidence that the beam is weak $X_9 \geq 1$, i.e. $P = P(X_1 \geq 1 | X_9 \geq 1)$. The CPM best estimates provided in Table 5 are randomly perturbed using Gaussian laws truncated at zero (with mean correspond to the values given in Table 5, standard deviation of 0.2 for the regression coefficients and of 0.5 for the intercept terms). In total 43 variables are considered.

Table 4: Definition of the CPT entry in the concrete BBN.

Node	Description
X_1	Damage assessment
X_2	Cracking state
X_3	Cracking state in shear domain
X_4	Steel corrosion
X_5	Cracking state in flexure domain
X_6	Shrinkage cracking
X_7	Worst cracking in flexure domain
X_8	Corrosion state
X_9	Weakness of the beam
X_{10}	Deflection of the beam
X_{11}	Position of the worst shear crack
X_{12}	Breadth of the worst shear crack
X_{13}	Position of the worst flexure crack
X_{14}	Breadth of the worst flexure crack
X_{15}	Length of the worst flexure cracks
X_{16}	Cover
X_{17}	Structure age
X_{18}	Humidity
X_{19}	PH value in the air
X_{20}	Content of chlorine in the air
X_{21}	Number of shear cracks
X_{22}	Number of flexure cracks
X_{23}	Shrinkage
X_{24}	Corrosion

Table 5: Definition of the CPM parameters of the concrete BBN; for instance m_{0_1}*, is the intercept of the regression model (Eq. 9) linking node* X_1 *to its parents;* Z_{1_9} *is the regression coefficient that models the relation between node* X_1 *and* X_9*;* s_{0_1} *is the corresponding standard deviation.*

Node	Intercept	Regression coefficient	Standard Deviation
X_1	$m_{0\_1}=0$	$Z_{1\_9}=0.3$	$s_{0\_1}=10^{-4}$
		$Z_{1\_2}=2$	
		$Z_{1\_10}=0$	
X_2	$m_{0\_2}=0$	$Z_{2\_5}=0.7$	$s_{0\_2}=10^{-4}$
		$Z_{2\_4}=0.5$	
		$Z_{2\_6}=0.3$	
		$Z_{2\_3}=0.7$	
X_3	$m_{0\_3}=0$	$Z_{3\_8}=0.3$	$s_{0\_3}=10^{-4}$
		$Z_{3\_21}=0.5$	
		$Z_{3\_12}=0.9$	
		$Z_{3\_11}=0.7$	
X_4	$m_{0\_4}=0$	$Z_{4\_5}=0.3$	$s_{0\_4}=10^{-4}$
		$Z_{4\_24}=0.7$	
		$Z_{4\_8}=0.7$	
X_5	$m_{0\_5}=0$	$Z_{5\_22}=0.5$	$s_{0\_5}=10^{-4}$
		$Z_{5\_7}=0.9$	
		$Z_{5\_13}=0.7$	
X_6	$m_{0\_6}=0$	$Z_{6\_23}=0.3$	$s_{0\_6}=10^{-4}$
		$Z_{6\_8}=0.7$	
X_7	$m_{0\_7}=0$	$Z_{7\_17}=0.4$	$s_{0\_7}=10^{-4}$
		$Z_{7\_16}=0.4$	
		$Z_{7\_15}=0.6$	
		$Z_{7\_14}=0.6$	
		$Z_{7\_8}=0.6$	
X_8	$m_{0\_8}=0$	$Z_{8\_20}=0.8$	$s_{0\_8}=10^{-4}$
		$Z_{8\_19}=0.9$	
		$Z_{8\_18}=0.5$	

Figure 13A depicts the evolution of the R^2 indicators considering the different residuals' formulations. This shows that a minimum of 2,000 random perturbations is required to consider the BBR model adequate with R^2 values above 98%. This is also confirmed by the visual inspection of the normal Q-Q plot in Figure 13B-D.

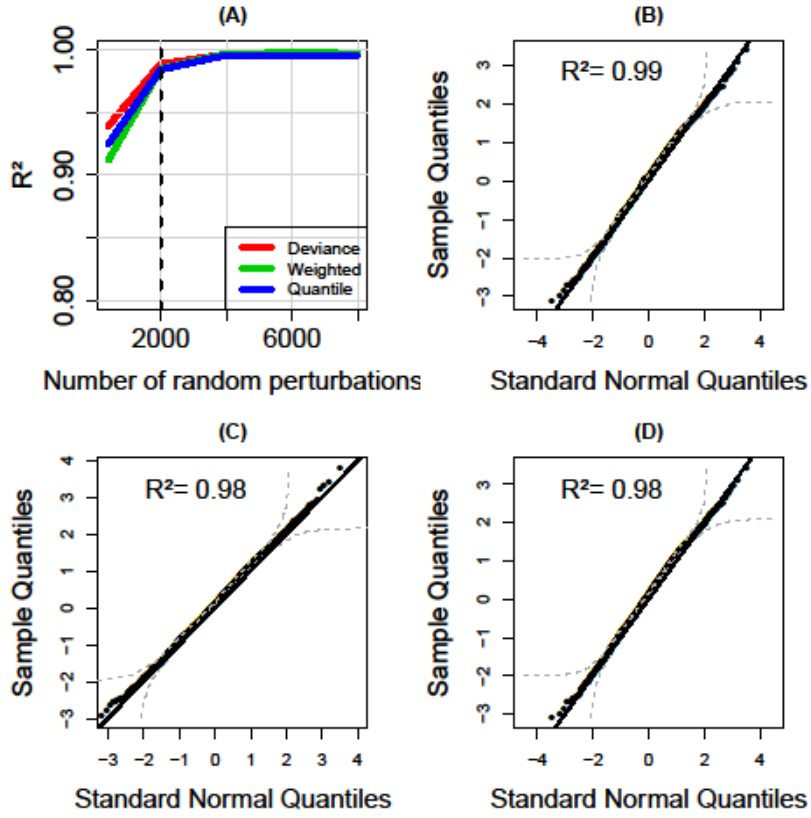

Figure 13: (A) Evolution of the R^2 indicator as a function of the number of random perturbations for the reinforced-concrete BBN. Three residuals' formulations are considered (see Appendix D). The vertical dashed line indicates the selected number of random perturbations. For this number, normal Q-Q plots are provided considering different residuals: (B) deviance; (C) standardized weighted; (D) quantile. The dashed lines indicate the boundaries of the 95% confidence band based on the Kolmogorov-Smirnov statistic (Doksum and Sievers, 1976). The value of the R^2 indicator (Eq. 13) is also reported.

Figure 14A depicts the corresponding histogram of the randomly generated *P* values (with mean of 0.8 and standard deviation of 0.08). Figure 14B shows that the Beta mean is very informative with a good agreement with *P*. The optimal stopping iteration of the regression model is selected based on a 5-fold cross validation procedure combined with the noncyclic algorithm as illustrated in Figure 14C.

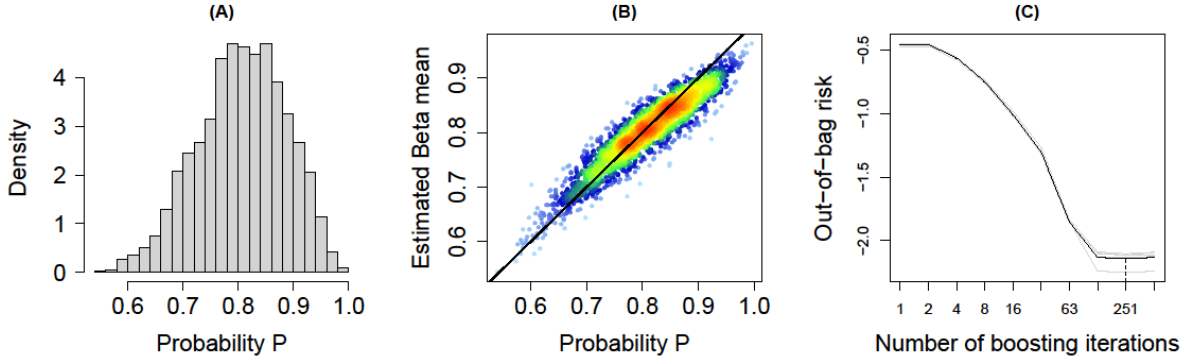

Figure 14: (A) Histogram of randomly generated P values for the concrete network; (B) Comparison between the estimated Beta mean and P (the colours indicate the density of the dots); (C) Evolution of the (out-of-bag) risk estimated using a 5-fold cross-validation procedure as a function of the number of boosting iterations; the optimal stopping iteration is selected as the one minimizing the average risk over all 5 cross-validation iterations (indicated by a vertical dashed line at 251).

The number of parameters of the conditional probability model is larger (almost four times) than the case described in Sect. 4.3. In this case, despite the regularisation associated to the boosting algorithm, the resulting BBR model can still remain too rich to be easily interpretable by BBN practitioners. The direct application of the boosting algorithm ends up here with more than 30 variables, i.e. analysing each of the partial effect may here not be practical. Therefore, the analysis is completed by the stability selection analysis (described in Appendix C) to further screen the most influential variables in the BBR model. Figure 15A depicts the selection probabilities for each CPM parameter with a threshold at 0.8 (see parametrisation in Appendix C). This shows that only the intercept terms for node X_2, X_5 and X_8 appear to be influential with respect to the Beta mean μ, whereas only the intercept terms for node X_2, X_3, X_5, X_7 and X_8 appear to be influential with respect to the Beta parameter σ. Interestingly, the nodes which affect the probability of interest are not necessarily the ones in direct connections with X_1 (see Figure 12).

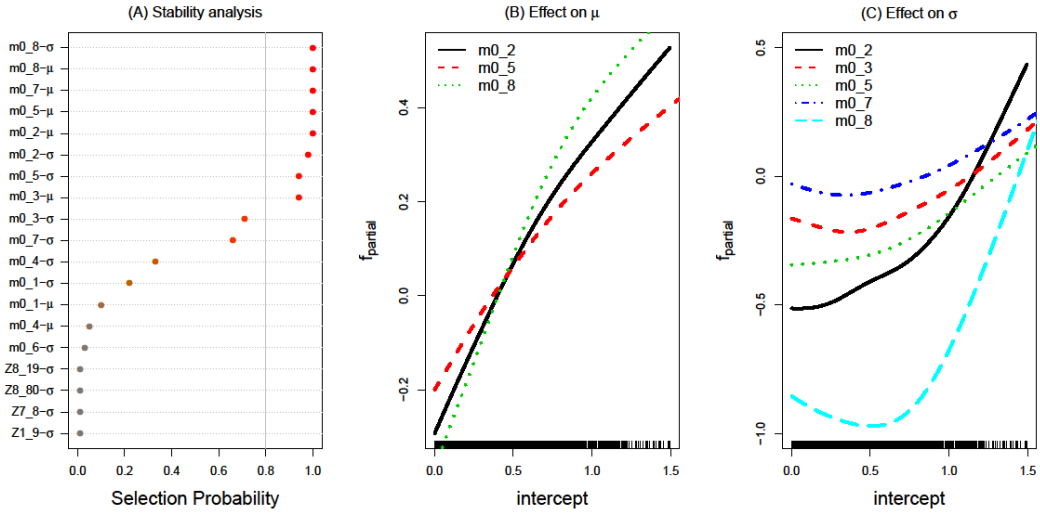

Figure 15: (A) Selection probability for each CPM parameter of the concrete network derived from the stability selection analysis (Appendix C). (B) Partial effect of the intercept m0 of nodes X_2, X_5 and X_8 on μ. (C) Partial effect of the intercept m_0 of nodes X_2, X_3, X_5, X_7 and X_8 on the σ parameter (logit-transformed).

The non-linear effects for each selected CPM parameters are depicted in **Erreur ! Source du renvoi introuvable.**B,C. This shows that the individual effect mainly corresponds to an increasing monotonic functions considering both parameters of the Beta distribution; with a higher nonlinear effect of m_0 of node X_8. This is confirmed by the Beta distribution's evolution with respect to the intercept parameter of node X_2 and X_8.

- Figure 16A shows that the increase of m_{0_2} mainly affects the increase of the best estimate of *P* (with only slight effect on the dispersion), whereas Figure 16B both affects the best estimate and the dispersion, i.e. the larger m_{0_8}, the larger the mean value of *P* (i.e. the riskier the situation), but also the larger the uncertainty on *P* (i.e. the occurrence of the risky situation remains uncertain);
- Figure 16C shows the evolution of the Beta's distribution when both parameters are increased similarly: we see that the combined increase amplifies the translation of the Beta's distribution to very high values, i.e. risky situations (driven by both increasing effects as shown in Figure 16B). Despite the increase in σ during this process, the occurrence of this risky situations remains of moderate-to-high confidence, which suggests that changes in m_{0_8} and m_{0_2} might ultimately lead to the failure of the concrete system.

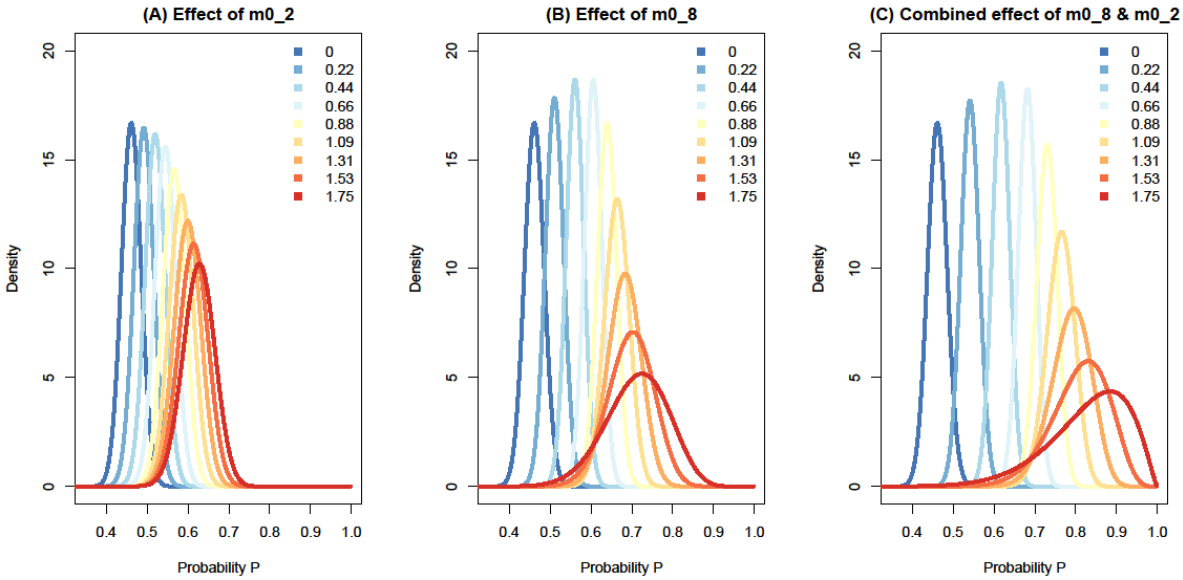

Figure 16: (A) Evolution of the Beta law fitted to the P values given increasing values of the intercept m_0 of node X_2 from low (0.) to high values (1.75); (B) Evolution of the Beta law fitted to the P values given increasing values of the intercept m0 of node X_8 from low (0.) to high values (1.75); (C) Evolution of the Beta law fitted to the P values given increasing values (with same increment) of both intercepts.

4.4.2 BBN-based reliability assessment

Figure 17 depicts the BBN constructed by Gehl and Rohmer (2018) for studying the problem of station blackout (node SYS) following an earthquake at a given nuclear power plant (NPP) sub-system in NARSIS WP2. The earthquake event is characterized by two intensity measures (nodes IM1 and IM2 respectively corresponding to the peak ground acceleration and the spectral acceleration at the first vibration period of the structure). The NPP sub-system is composed of a 5-story reinforced-concrete structure hosting two emergency diesel generators (EDGs). Three damage events (STR for structural damage and EDG for failure of the anchorage of the generators) are considered.

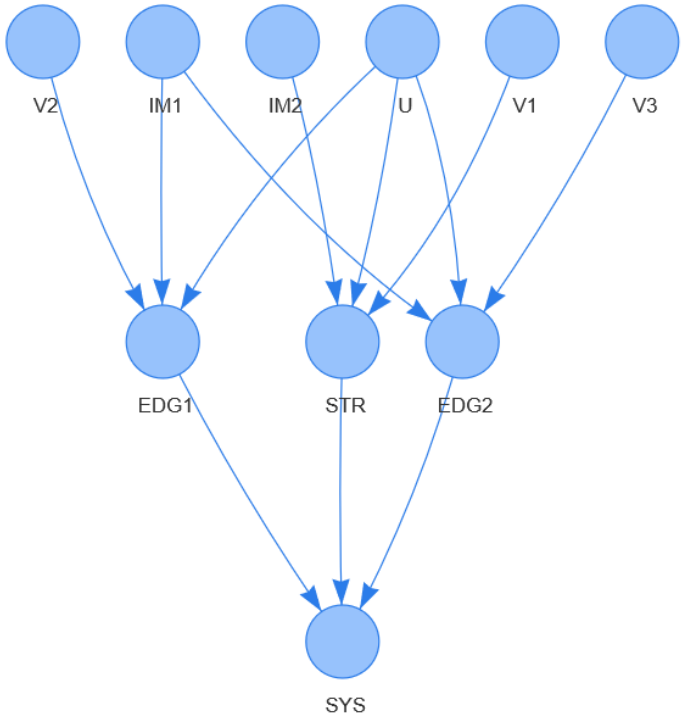

Figure 17: Structure of the network for studying the NPP subsystem reliability; IM1 and IM2 are deterministic nodes representing intensity measure characterizing the earthquake event; Nodes U, V1, V2 and V3 are zero-centered Gaussian random variables used to incorporate correlation. Only the sensitivity to the parameters for the blue nodes is investigated.

The conditional probabilities of the failure states of STR, EDG1 and EDG2 are estimated through fragility functions (i.e. probabilistic model that relates the failure probability to the intensity measure IM), which are derived from non-linear seismic time histories applied to the structure. Due to the observed statistical dependence between the failure events (i.e., due to the common seismic loading applied to the three components), auxiliary variables U, V1, V2 and V3 (described by a standard normal distribution) are added to the BBN following the approach by Gehl and D'Ayala (2016). These variables result from the Dunnett-Sobel decomposition of the correlation coefficients between the safety factors of the components as follows:

$$Z_i = t_i \cdot U + \sqrt{1 - t_i^2} \cdot V_i \quad \text{(Eq. 14)}$$

where Z_i is the standard score of the safety factor of component *i* (Z_1 corresponds to STR, Z_2 to EDG1, and Z_3 to EDG2) and t_i is the Dunnett-Sobel coefficient that approximates the correlation between the failure events.

By definition, the failure of component *i* occurs if $Z_i \leq -\beta_c$, where β_c is the reliability index expressed as follows:

$$\beta_c = \frac{\alpha_i - \ln im}{\beta_i} \quad \text{(Eq. 15)}$$

where α_i and β_i are the fragility parameters (median and standard dispersion) of component *i*, under the common assumption of a cumulative lognormal distribution for the fragility function; *im* is the value of the intensity measure of interest (IM1 for EDG1 and EDG2, IM2 for STR, see Figure 17).

Based on this framework, the CPT of the failure event of a component *i* is built by considering all combinations of discretized values {*im*; *u*; v_i}, and by checking the following condition (Gehl and D'Ayala, 2016):

$$\left(z_i = t_i \cdot u + \sqrt{1 - t_i^2} \cdot v_i\right) \leq -\frac{\alpha_i - \ln im}{\beta_i} \quad \text{(Eq. 16)}$$

For the sensitivity analysis, we do not consider the value of the CPT entries directly but the physical parameters, which determine them, namely the parameters of the fragility curves, (mean α and standard deviation β). The numerical values of the physical parameters considered in this application are detailed in Table 6. The fragility curves' parameters were randomly perturbed via a zero-centered Gaussian noise with standard deviation that is 10% of the original values (termed as CPM best estimates in the following). For the parameters of Dunnett-Sobel decomposition, the Gaussian noise is truncated at one. The probability of interest is here the probability of the sub-system failure, i.e. *P*=P(SYS=1) given an earthquake event characterised by intensity measures IM1 and IM2 of respectively 10 and 12.5 m²/s. In total, 9 parameters are considered.

Table 6: Parameters for constructing the CPT of the BBN-based reliability assessment

Parameter	Symbol	Original value
Mean and Standard deviation value of the log-normal fragility curve for STR	α_{STR}, β_{STR}	-6.48, 2.32
Mean and Standard deviation of the log-normal fragility curve for EDG1	α_{EDG1}, β_{EDG1}	-12.250, 6.22
Mean and Standard deviation of the log-normal fragility curve for EDG2	α_{EDG2}, β_{EDG2}	-4.66, 2.20
Dunnett-Sobel decomposition's parameters	$t_{1,2,3}$	0.914, 0.942, 0.999

The selection of the minimum number of random perturbations is more difficult than for the brain tumour or for the reinforced concrete case. Figure 18A shows that at least 1,000 random perturbations are necessary to reach R^2 values above 95%, but due to oscillations in the evolution of the R^2 values, we preferably choose the largest number, i.e. >4,000. The visual inspection of the normal Q-Q plots (Figure 18C-D) also reveals some deviations for very high and low quantiles (outside the range [-2 - 2]) though it should be noted that they remain within the 95% confidence band and with low-to-moderate magnitude. Contrary to the brain tumour case, the three residuals' formulations all agree on the identification of the problem. A deeper analysis shows that these deviations correspond here to Beta

distributions with very high mean and very low variance values: the sensitivity should be analysed with care for these cases.

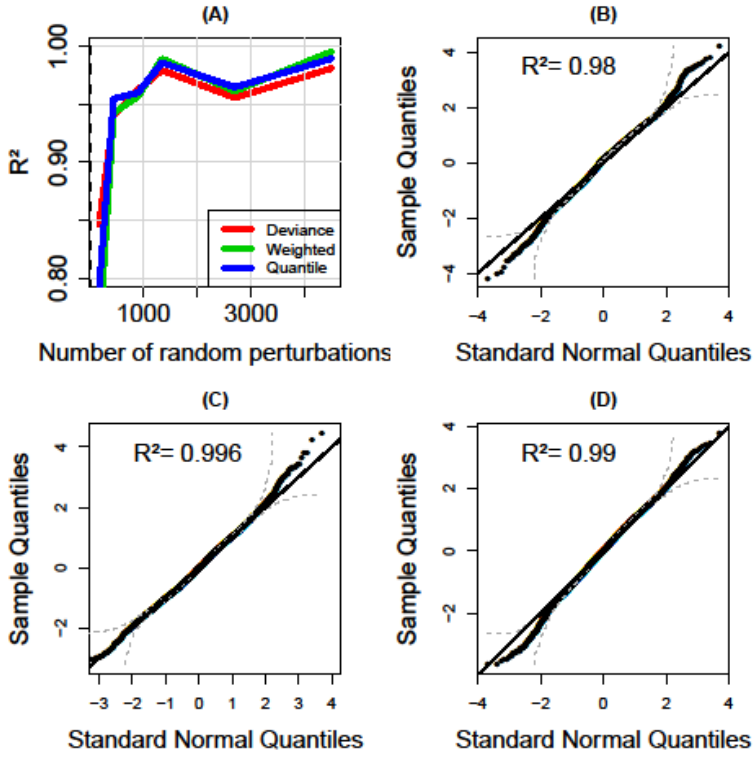

Figure 18: (A) Evolution of the R^2 indicator as a function of the number of random perturbations for the BBN-based reliability assessment. Three residuals' formulations are considered (see Appendix D). The vertical dashed line indicates the selected number of random perturbations. For this number, normal Q-Q plots are provided considering different residuals: (B) deviance; (C) standardized weighted; (D) quantile. The dashed lines indicate the boundaries of the 95% confidence band based on the Kolmogorov-Smirnov statistic (Doksum and Sievers, 1976). The value of the R^2 indicator (Eq. 13) is also reported.

The histogram of P values is provided in **Erreur ! Source du renvoi introuvable.**A with mean and standard deviation at respectively 0.65 and 0.26. Contrary to the reinforced-concrete BBN, the agreement with P is less satisfactory (**Erreur ! Source du renvoi introuvable.**B). A major part of the P values (see the warm colour indicating the density of dots in **Erreur ! Source du renvoi introuvable.**B) appear to be reproduced by the Beta mean, but the scatter plot remains disperse. This type of analysis can be considered a complement to the analysis of the Q-Q plots (Figure 18) and supports a cautious attitude with respect to the conclusions drawn from the sensitivity analysis. The optimal stopping iteration of the regression model is selected based on a 5-fold cross validation procedure combined with the noncyclic algorithm as illustrated in **Erreur ! Source du renvoi introuvable.**C.

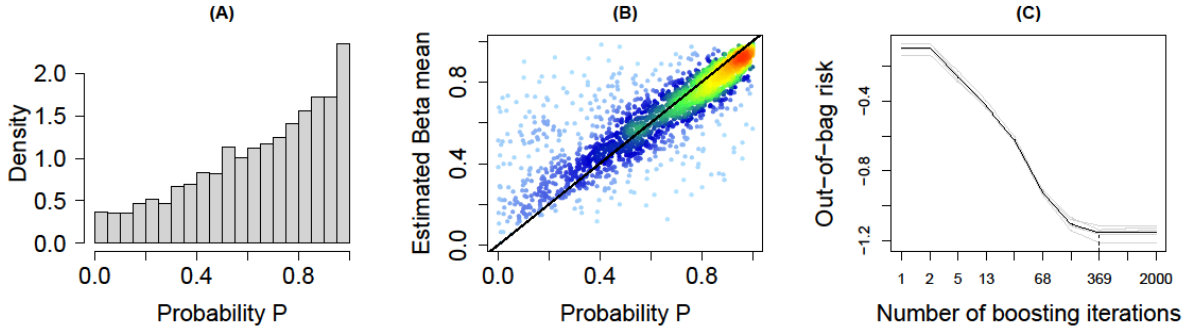

Figure 19: (A) Histogram of randomly generated P values for the NPP reliability network; (B) Comparison between the P values and the estimated mean value provided by the Beta model; (C) Evolution of the (out-of-bag) risk estimated using a 5-fold cross-validation procedure as a function of the number of boosting iterations; the optimal stopping iteration is selected as the one minimizing the average risk over all 5 cross-validation iterations (indicated by a vertical dashed line at 369).

The application of the boosting algorithm reveals that only the parameters of the fragility curves are selected. These are the only parameters identified as significant by the BBR approach, i.e. the correlation parameters $t_{1\text{-}3}$ are discarded by the algorithm. Figure 20 provides the corresponding partial effects for both Beta law parameters.

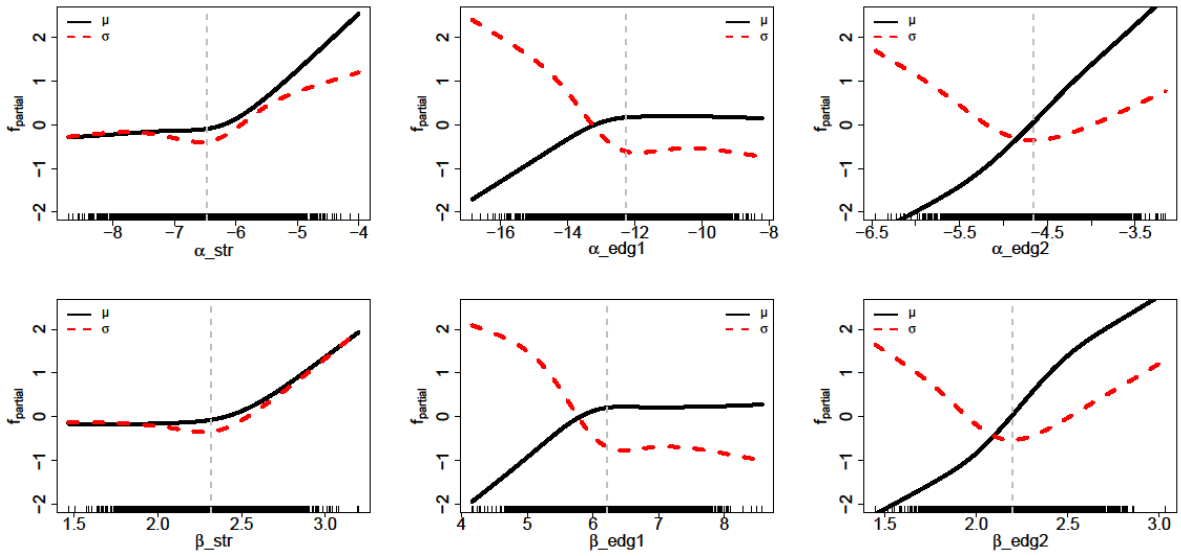

Figure 20: Partial effect of the fragility curve's parameters on μ (logit-transformed) (black straight line) and on □ (logit-transformed) (red dashed line). The vertical grey-coloured dashed line indicates the CPM best estimates of Gehl and Rohmer (2018).

Several observations can be made:

- The parameters (α_str, β_str) of the structural fragility curve (STR, Figure 20, left) have almost similar effect, whatever the Beta law parameter; it corresponds to a quasi- bilinear function, which remains quasi-constant below the CPM best estimate then increases above it; from a risk viewpoint, this means that the damage to the structure enhances the occurrence of risky situations, where the system failure's probability *P* might reach high values. Yet, the effect on σ parameter also indicates that the confidence in the occurrence of this probabilistic regime is low;
- The effects of the parameters (α_edg2, β_edg2) of the second electrical generator's fragility curve (EDG2, **Erreur ! Source du renvoi introuvable.**, right) are quasi-linear with respect to the Beta law mean μ, but is non-monotonic with respect to the σ parameter. This can be schematically understood as a decrease of uncertainty on *P* (i.e. the Beta law dispersion) when approaching the original value, then an increase above it;
- The effect of the parameters (α_edg1, β_edg1) of the first electrical generator's fragility curve (EDG1, Figure 20, center) is more complex. The effect on the Beta mean μ corresponds to a bilinear function, which increases at around the CPM best estimate, then remains quasi-constant above it (i.e. to a lesser extent, it corresponds to the opposite behaviour to the one for STR). The effect on the Beta parameter σ corresponds to an inverted sigmoid, which reaches its lower horizontal plateau above the CPM best estimate. This means that above their original values, parameters (α_edg1, β_edg1) little affect the system failure's probability.

Figure 21 illustrates how α_str, α_edg1 and α_edg2 act differently on the system failure. When increasing α_str, the system failure starts increasing only for values well above the CPM best estimates. This is shown by the Beta distributions, which remains "stuck" at moderate values (around 0.6; see for cold colours in Figure 21A). When increasing α_edg1, the resulting Beta distribution remains stuck at high value around 0.70-0.75 (note the evolution of the mode for warm colours in Figure 21B), hence leading to risky situations. The confidence in the occurrence of such probabilistic regime is high as indicated by the low dispersion of the Beta distributions. When increasing α_edg2, the Beta distribution continues to translate towards very high values above 0.90. Despite the very low dispersion of the Beta distribution, the confidence remains here moderate, because this situation corresponds to the one for which the normality of the residuals is not met (Figure 18).

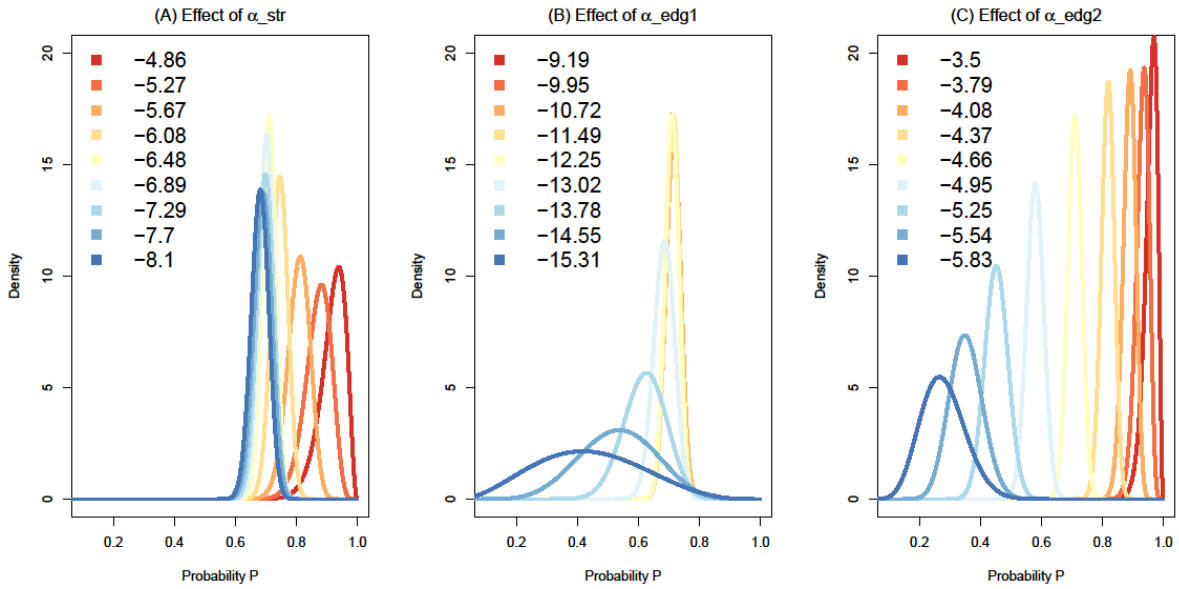

Figure 21: Evolution of the Beta distributions fitted to the P values given: (A) increasing values of the mean value of the fragility curve α_str; (B) increasing values of α_edg1; (C) increasing values of α_edg2.

4.5 Discussion

Ensuring the validity and credibility of increasingly complex BBN-based expert systems (Pitchforth & Mengersen, 2013; Kleemann et al., 2017; Marcot and Penman, 2019) requires a broad vision on the sensitivity to the CPM parameters. As outlined in the introduction, the most widely used approach is based on sensitivity functions for discrete BBNs, and on partial derivatives for continuous BBNs. Reasons are the intuitive interpretation of the results (thanks to the graphical presentation) and the simplicity of the implementation. Yet, these approaches only provide information on the local influence, in the sense that the parameters are varied “one-at-a-time”. This means that it can only provide a restricted vision on sensitivity, because the exploration of the sensitivity remains limited to a few CPM parameters, while the domain of the other CPM parameters is left mostly unexplored (as thoroughly discussed by Saltelli et al. (2019) with respect to sensitivity analysis practices). Multi-way SA methods have been proposed (Leonelli et al., 2017; Gómez-Villegas et al., 2013), but they can rapidly become intractable.

In this context, the proposed BBR approach can be considered more complete by providing global insight on the sensitivity by means of the partial effects, which directly show the individual, possibly non-linear, effects of all CPM parameters. In Sect. 4.4, we have shown how the BBR approach can provide richer information than existing methods at multiple levels:

- Level (1): it selects the most influential parameters and it screens those that are of negligible influence (information that is generally unknown a priori);
- Level (2): it provides the functional relation between the CPM parameters and the result of the probabilistic query. The proposed approach builds on a graphical presentation of the results, which eases the interpretation;
- Level (3): the practitioner can study how the combined effect of the CPM parameters can lead to different probabilistic regimes (e.g., situations of high probability values) by studying the evolution of the Beta mean. Furthermore, the practitioner can measure the confidence in the occurrence of the identified probabilistic regimes, by studying the effect on the Beta σ parameter.

Table 7 provides a summary of the strengths and weaknesses of the BBR approach with comparison to the approach based on sensitivity functions.

Table 7: Summary of the strengths and weaknesses of the BBR method and of the approach based on sensitivity functions.

Approach	Strengths	Weaknesses
Sensitivity function	It is simple to implement; It requires a low computational effort; The graphical representation is straightforward to interpret.	It is local: it focuses on the influence of one (or multiple) CPT parameter while the other ones are kept constant; It is restricted to the analysis of discrete BBNs; Multi-way SA can rapidly become intractable.
BBR	It provides insight in the global influence; It is simple to implement using random sampling, which is a generic procedure applicable to any types of BBNs; The results are intuitive to interpret based on a graphical presentation; It provides multilevel information on sensitivity; The combination of gradient boosting and stability selection increases the robustness to the number of parameters.	The number of calls to the BBN inference engine can be large (>1,000); The adequacy of the Beta model should be carefully checked; The demonstration of the applicability to very large-scale BBNs with hundreds of nodes and thousands of CPM parameters remains to be done.

From an operational viewpoint, we tested the applicability of the BBR approach using different application cases covering a large spectrum of situations, namely (1) a small discrete BBN, used to capture medical knowledge, to exemplify the functionalities; (2) a linear Gaussian BBN, used to assess the damage of reinforced concrete structures, exemplifies a case where the number of parameters is too large to be easily processed and interpreted (>40 parameters); (3) a discrete BBN, used for reliability analysis of nuclear power plant, exemplifies a case where analytical solutions for sensitivity can hardly be derived. To ease the implementation, we proposed a procedure based on random experiments, i.e. the BBN-based results are derived from randomly generated values of the CPM parameters. This procedure is generic, because it can be applied to any set of CPM parameters whatever the type of the considered BBN: discrete (with CPT entries), continuous (with regression coefficients), or hybrid.

However, it should be underlined that providing information on the global effect of the CPM parameters comes at the expense of a larger computational effort and complexity. The number of calls to the BBN inference engine is larger (typically >1,000) compared to the sensitivity functions, which may become problematic when the inference is difficult (hence time consuming) to perform.

The pillar of the BBR approach is the adequacy of the BBR model to explain the BBN-derived probabilities. This adequacy should be carefully checked, and we propose here to investigate the statistics of the residuals. In some situations, this might reveal situations where the interpretation should be conducted with care as exemplified by the third application case. The difficulties encountered for this case is also related to the characteristics of the sensitivity analysis. Contrary to the brain tumour and to the reinforced concrete BBN, this case does not consider the value of the CPM parameters directly, but the physical parameters that influence them. This adds a level of complexity to the problem and make the BBR model more difficult to fit.

Finally, it should be noted that the second application case shows that the BBR approach is robust even in the presence a large number of parameters (which can rapidly grow as a function of the number of BBN nodes). Yet, the applicability to complex cases with several hundreds of nodes (and thousands of parameters), like the pathfinder network (Heckerman et al., 1992), remains an open question especially regarding two aspects: (1) the capability of the combined “gradient boosting - stability selection analysis” to handle so many terms; (2) the complexity of the interpretation of the partial effects.

4.6 Summary and future research directions

The rapidly increasing advances of BBN for modelling of expert systems (and for NARSIS project in particular) calls for the developments of robust methods for their validation and verification (e.g., Marcot and Penman, 2019). One major pillar to fulfil this purpose is sensitivity analysis. The proposed BBR approach broadens the scope of existing BBN sensitivity analysis methods by providing a larger vision (global) on the CPM influence. The approach has the advantage of being generic (it can be applied to any kind of BBN, i.e. discrete, Gaussian or hybrid), and robust to the number of parameters (that can rapidly increase, typically reaching several dozens, even for moderate number of BBN nodes).

Bringing the BBR approach to a fully operational state, raises different questions that should be addressed in future work. The first line of future research should concentrate on the intensification of the applicability tests using very large-scale BBNs. An important aspect to be tested is the applicability to highly constraining situations where the number of variables largely exceeds the size of the training database. In such cases, the performance of the stability selection analysis should be more extensively investigated (see Meinshausen & Bühlmann, 2010; Thomas et al., 2018). The second research direction should concentrate on improving the interpretability of the results. The graphical representation of the partial effects is a strength of the BBR approach but might lose its conciseness as the number of functional terms selected as important largely increases (>100). We should take advantage of advances in distributional regression methods that rely on trees like the one proposed by Grün et al. (2012) for Beta regression. The presentation of the results using a network is expected to provide a more concise and understandable presentation of the results. Finally, it should be underlined that the current work has focused on only one part of the problem of uncertainties in BBNs. The CPM parameters constitute only one ingredient for BBN development; the second one being the Directed Acyclic Graph (DAG) specification, which has its own challenges as well, in particular when the learning is based on data (see e.g., a comprehensive review by Heinze-Deml et al., 2018). To address the whole spectrum of uncertainties in BBN building, sensitivity methods both covering DAG and CPM learning would be beneficial. Again, a solution relying on trees is worth investigating, as recently proposed to deal with psychometric networks (Jones et al., 2019).

5 Uncertainty reduction in fragility assessments

With the objective of characterizing uncertainty pervading NARSIS models, we specifically address the question of components' fragility for the main NPPs critical elements, more specifically the question of uncertainty management of these fragility assessments. The objective is to constrain the uncertainty of fragility curves that constitute key tools for NARSIS project (and for WP2 in particular). In this view, we propose a strategy for uncertainty reduction by relying on Bayesian framework (e.g. Straub & Der Kiureghian, 2008; Wang et al, 2018b). The methodology is tested on an application for seismic risk analysis, but could easily be adapted to any hazard due to the versatility of the Bayesian setting.

5.1 Context and overall approach

Fragility curves characterize the reliability of structures and equipment as a function of seismic load level. Fragility curves are usually computed considering the log-normal distribution assumption. The interested reader can refer to deliverable D2.6 of NARSIS for further details.

The estimation of the parameters of the fragility curves requires to gather different sources of information and to quantify the uncertainties coming from these sources. Since a more accurate uncertainty quantification is not always possible, generic values are applied (EPRI 2009).

We present a **Bayesian updating framework** that allows for an improved seismic capacity estimation and possible reduction of uncertainties based on information from experience feedback.

Different sources of uncertainties are quantified and integrated in the computation of the fragility curves (see e.g. Der Kiureghian & Ditlevsen, 2009), namely:

- *Aleatory uncertainty/variability* (also referred to as randomness). The physical environment or engineered system under study can behave in different ways or is valued differently spatially or/and temporally. The aleatory variability is associated with the impossibility of predicting deterministically the evolution of a system due to its intrinsic complexity. Hence, this source of uncertainty represents the "real" variability and it is inherent to the physical environment or engineered system under study, i.e., it is an attribute/property. Examples are ocean fluid dynamics and the occurrence of earthquakes;
- *Epistemic uncertainty.* This type is also referred to as "knowledge-based", as the Greek term *episteme* means knowledge. In contrast to the first type, epistemic uncertainty is not intrinsic to the system under study and can be qualified as being "artificial", because it stems from the incomplete/imprecise nature of available information, i.e., the limited knowledge of the physical environment or engineered system under study.

In terms of uncertainty management, aleatory uncertainty, being a property of the system under study, cannot be reduced. However, concrete actions can be taken to increase overall capacity of the structure or system under consideration. A good illustration is the reinforcement of protective infrastructures such as the height of dykes to counter in a preventive fashion the temporal variations in the frequency and magnitude of storm surges. Another option can be based on the application of an additional "safety margin" for the design of the engineered structure. On the other hand, epistemic uncertainty, being due to the capability of the analyst (measurement capability, modeling capability, etc.), can be reduced by, e.g., increasing the number of tests, improving the measurement methods or evaluating calculation procedure with model tests.

In this study, we focus on reduction of epistemic uncertainty by means of damage data, collected from the in-situ observation and the database of the seismic qualification utility group (SQUG). These are used to construct the likelihood function for the Bayesian update (Wang et al, 2018b). The posterior equipment capacity is evaluated by Markov Chain Monte Carlo (MCMC) simulation (Hastings, 1970) and posterior fragility curves are, then, obtained. The methodology is applied to compute the fragility curves of a low-voltage switchgear of a nuclear power plant, within the so-called KARISMA benchmark (IEAE, 2014).

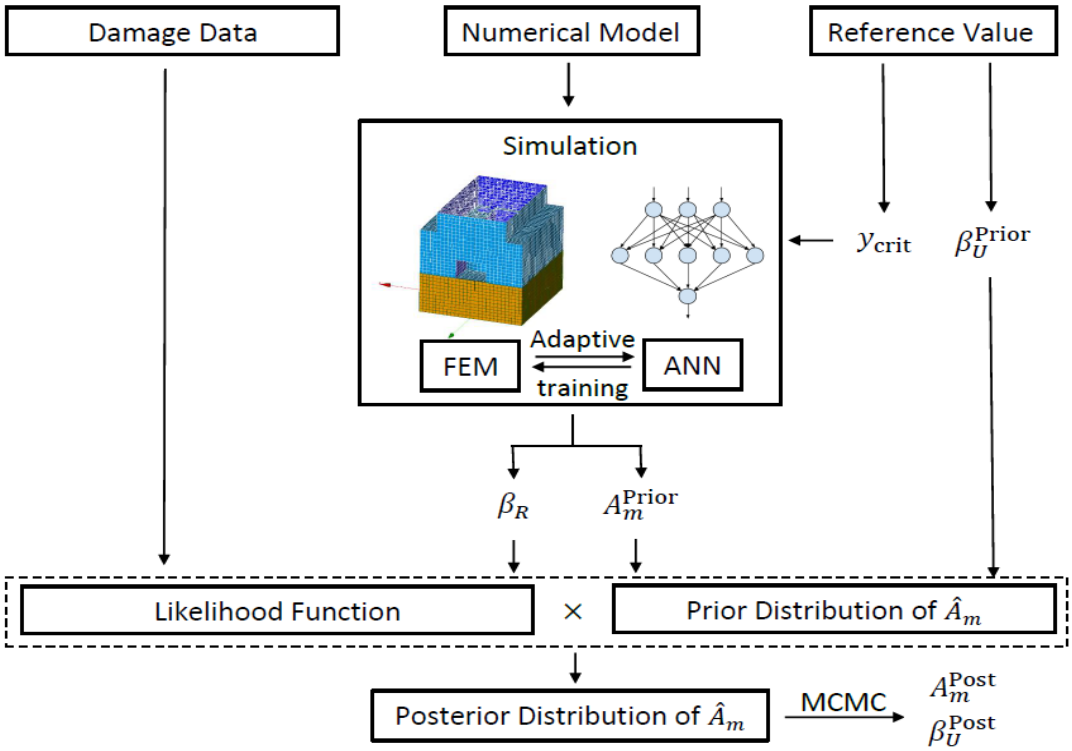

Figure 22: Overview over approach adopted for Bayesian updating of fragility curves parameters (Wang et al, 2018b)

5.2 Bayesian updating of fragility curves

Fragility curves compute the conditional probability that the damage measure (DM) exceeds a failure threshold, for a given seismic Intensity Measure denoted here α:

$$P_f(\alpha) = \mathbf{\Phi}\left(\frac{\ln \alpha - \ln \hat{A}_m}{\hat{\beta}_R}\right) \quad \text{(Eq. 17)}$$

Where $\hat{A}_m$ is the median capacity, and $\hat{\beta}_R$ is the logarithmic standard deviation representing aleatory uncertainty related mainly to uncertain seismic load for a given intensity level and material properties. In the Bayesian framework, these two parameters are modelled as lognormal random variables: $\hat{A}_m \sim LogN(A_m, \beta_U^2)$, $\hat{\beta}_R \sim LogN(\beta_R, \beta_{R_r}^2)$.

The state x^i of equipment i after the seismic event is modelled by a Bernoulli random variable:

$x^i = 1$, failure occurs;

$x^i = 0$ otherwise.

Then the likelihood function L reads as follows:

$$L\left(\mathbf{z}|\hat{A}_m, \hat{\beta}_R\right) = \prod_{i=1}^{N} [P_f(\alpha^i)]^{x^i} [-P_f(\alpha^i)]^{1-x^i} \quad \text{(Eq. 18)}$$

where N is the number of observations.

By applying Bayes theory, the posterior distribution of $\hat{A}_m$ and $\hat{\beta}_R$ reads:

$$f\left(\hat{A}_m, \hat{\beta}_R|\mathbf{z}\right) = cL\left(\mathbf{z}|\hat{A}_m, \hat{\beta}_R\right) LogN(A_m, \beta_U^2) LogN\left(\beta_R, \beta_{R_r}^2\right) \quad \text{(Eq. 19)}$$

where c is a normalizing constant for $f\left(\hat{A}_m, \hat{\beta}_R|\mathbf{z}\right)$. We suppose here that $\hat{A}_m$ et $\hat{\beta}_R$ are independent variables in order to obtain the expression for the updated distribution of the two variables.

The overall approach for Bayesian updating of fragility curves is illustrated in Figure 22. The methodology consists in the:

i) estimation of the prior parameters A_m and β_R with numerical simulations: to reduce the computational cost, an Artificial Neural Network (denoted ANN in Figure 22) metamodel (e.g., Aggarwal, 2018) is trained with an iterative active learning algorithm to substitute the computationally expensive Finite Element Model (denoted by FEM in Figure 22) simulation as described by Wang et al, (2018a). Generic values are used for β_U prior modelling epistemic uncertainty.
ii) computation of the likelihood function with the damage data and execution of Bayesian updating to obtain the posterior distribution of the seismic capacity of the equipment.

Note that further implementation details on meta-modelling techniques are available in NARSIS deliverable D4.2.

5.3 Application to Kashiwazaki Kariwa (KK) NPP

5.3.1 Study case

In 2007, the Kashiwazaki-Kariwa nuclear power plant (K-K NPP) experienced an earthquake of magnitude 6.6, distance 16km. In this context, the KAshiwazaki-Kariwa Research Initiative for Seismic Margin Assessment (KARISMA) benchmark was organized by the International Atomic Energy Agency (IAEA, 2014).The prior estimation of fragility curve parameters has been carried out by EDF using numerical models established in the framework of this benchmark.

The equipment of interest is a low-voltage switchgear (LVSG) in the Kashiwazaki-Kariwa NPP (K-K NPP). In NPPs, the LVSG is a combination of electrical control units such as circuit breaks and relays, etc., whose function is to ensure and protect the performance of 480 V-AC (alternative current) electrical systems. We consider here fictitious LVSG located on floor -1. The damage or failure indicator is the average floor spectral acceleration in the range 5 Hz to 9 Hz. It is assumed that failure occurs for floor spectral accelerations above 1.8 g.

5.3.2 Database

The damage data used in this study are taken from the seismic qualification utility group (SQUG) database. The SQUG database (www.epriq.com/ewww.epriq.com/esqug/squg/), built by the Electric Power Research Institute (EPRI), gathers seismic experience data related to seismic capacity of equipment in industrial facilities (not limited to NPPs). The data in the SQUG database are mostly obtained from post-earthquake inspections of equipment in these industrial facilities. Thirty-two earthquakes from 1971 to 2010 are registered in the SQUG database with most of them taking place in the USA. Some strong earthquakes in various locations (Chile, Japan, Turkey, etc.) are also included. The equipment in the SQUG database is divided into 20 conventional classes, including switchgears, batteries, motor control centers.

For the data collected in the SQUG database, each observation contains the information:

i) equipment description (size, manufacturer, etc.);
ii) the earthquake and the PGA;
iii) the industrial facility where the equipment is located;
iv) the elevation *h* of the equipment in the facility structure;
v) the description of the performance of the equipment after the earthquake.

It has to be mentioned that no details on the supporting structures are provided in the database.

In our study, the damage data for the low-voltage switchgear from the SQUG database is used. A major issue in using experience feedback damage data is the fact that in-situ observation data bases provide peak groung acceleration (PGA) and information on equipment failure for the site and floor height of the on-site structure while the target equipment is generally located at a different level and this has a major impact on the demand. This is why a transformation of the data, as illustrated in Figure 23 for SQUG database, has to be carried out:

- From the free field PGA, the demand on the floor is deduced using a simple formula where the amplification of PGA is a linear function of height $\lambda_1(h)$ (EPRI 2014)

- This demand is taken as the demand experienced by the target structure.
- The corresponding PGA for the target structure is deduced by means of a floor amplification parameter λ_2 linking free field motion to floor acceleration. The latter is determined by the FEM model available for the target structure (here K-K NPP).

This yields the following relation to determine PGA at target site:

$$PGA_3 = PGA_1 \lambda_1(h)\ 1/\lambda_2 \quad \text{(Eq. 20)}$$

In the above expression PGA_3 designs the spectral acceleration at location (3) and α_1 is the value given for the observation in the database.

In both transformations, uncertainty is accounted for as described with more detail in Wang et al. (2018b). The uncertainty from the transformation is added to the fragility curve expression as an additional $\beta^2_{1\to3}$:

$$P_f(\alpha) = \Phi\left(\frac{\ln \alpha_3 - \ln \hat{A}_m}{\sqrt{\beta_R^2 + \beta^2_{1\to3}}}\right) \quad \text{(Eq. 21)}$$

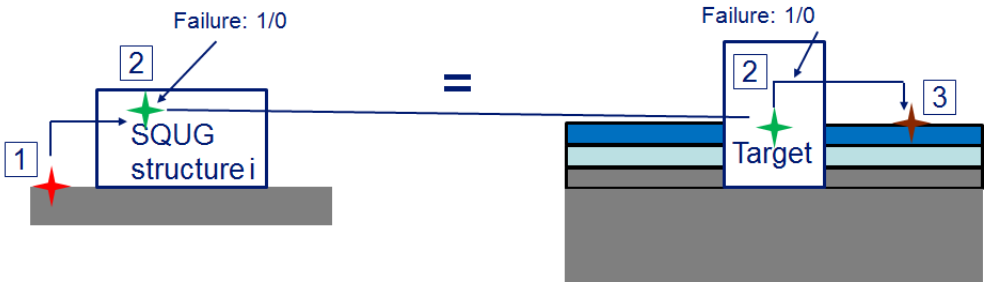

Figure 23: Transformation applied to obtain respective PGA at target structure (3), given the observation (1).

The total number of SQUG damage data for the LVSG is 78, with only one failure observed in the El Centro Steam Plant after the 1979 Imperial Valley Earthquake with local PGA value of 0.43 g. After the earthquake, it has been noticed that circuit breakers of the LVSG had refused to close. The local PGA values measured at different power plants are plotted in Figure 24. However, according to the inspection report, it is not clear that the functional failure of the LVSG is caused by the earthquake. It can be also due to the corrosion in the mechanical linkages, which is not earthquake-related. This is why we adopted a fractional x_i value 0.5 for the potential failure case of El Centro steam plant. It can be regarded as two realizations of earthquake observations, with one failure and one surviving.

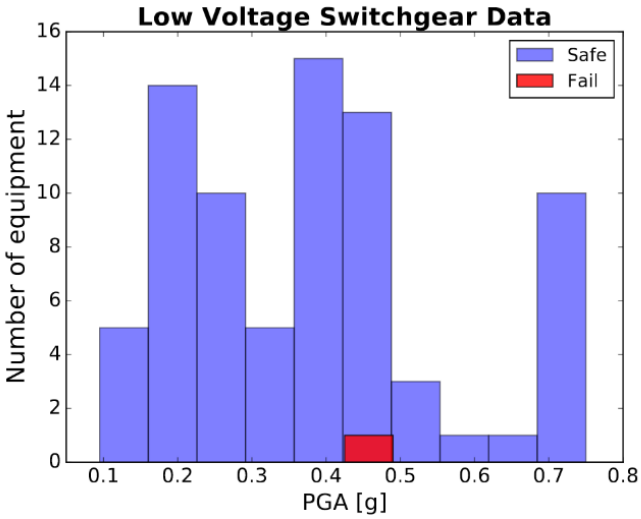

Figure 24: Damage data for low voltage switchgear from SQUG.

5.3.3 Results

The posterior distribution of the capacity is shown in Figure 25 on the left side. The resulting updated family of fragility curves is shown on the right side of Figure 25.

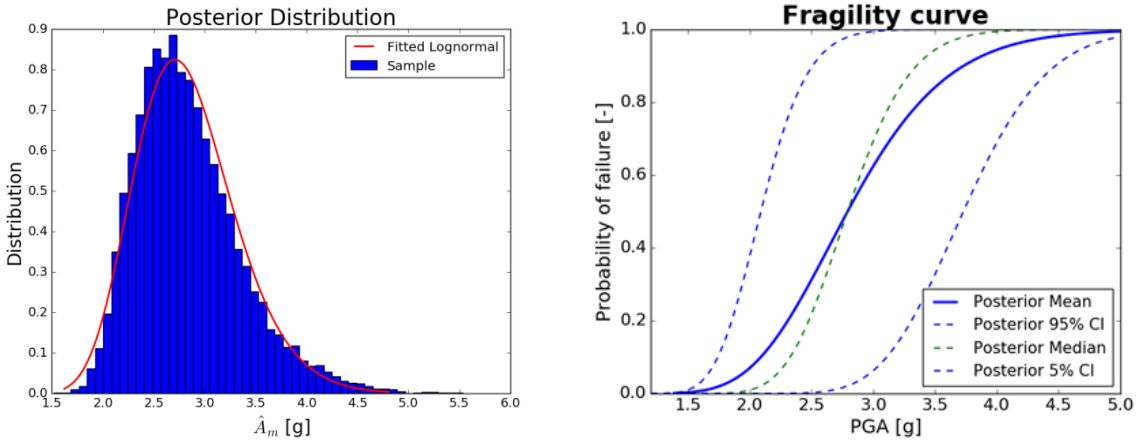

Figure 25: Posterior distribution (left) and updated fragility curves (right).

The prior and posterior estimates of the fragility curve parameters obtained for our example application are given in Table 8.

Table 8: Prior and posterior estimates of fragility parameters

β_R	A_m^{prior}	β_U^{prior}	$A_{\text{HCLPF}}^{\text{prior}}$	A_m^{post}	β_U^{post}	$A_{\text{HCLPF}}^{\text{post}}$
0.145	2.46g	0.4	1.00g	2.7g	0.176	1.59g

The application study for K-K NPP shows that, after the Bayesian updating, the median capacity has increased, due to few failure cases in the SQUG database while the epistemic uncertainty represented by β_U is reduced by >50% due to additional information from the SQUG data.

Finally, we also show that the High Confidence Low Probability Failure capacity (HCLPF) is largely increased (by 0.59g) after the Bayesian updating mainly due to the reduction of the epistemic uncertainty.

5.3.4 Implications for NARSIS

We can conclude that the afore-described methodology combining an ANN adaptive training algorithm with the amplification-factor-based construction of the likelihood function provides a valuable tool to reduce epistemic uncertainties (i.e. related to the lack of knowledge also named the reducible part of uncertainty) in the fragility curves (as the ones used in NARSIS).

The application of the methodology was restricted to a seismic risk analysis, but it should be underlined that the framework is flexible enough to be extended to other hazards (and associated fragility curves), in particular because of the versatility of the Bayesian setting. Second, the application takes advantage of the availability of the SQUG database but could easily be applied to any inspection data coming for instance from in site monitoring exercises for instance. This could constitute a valuable basis for NARSIS WP5 for instance.

6 Summary and recommendations

The present report D3.3 addresses the question of constraining the uncertainties in the components' modelling (causes and consequences). Both WP1 and WP2 involve complex models for respectively characterizing the physical external threats and the vulnerability and integrity assessment of NPP system components. In practice, this imposes processing a large number of sources of uncertainty whether regarding parameter uncertainty, but also model uncertainty.

Building upon the recent best practices for uncertainty assessment (de Rocquigny et al. 2008, in collaboration with the European Safety Reliability Data Association), a special attention will be paid to characterize uncertainty pervading these models by adapting or developing techniques for sensitivity analysis, denoted SA (Iooss & Lemaître, 2015).

First, D3.3 aims at providing an overview of the existing techniques / methods in the field of nuclear safety analysis. This shows that sensitivity analysis is a crucial task of any nuclear safety analysis. Its use is not new (Sect. 3.3) and in the past, numerous techniques have been developed to address this question whether for a local (Sect. 3.1) or a global (Sect. 3.2) analysis. A detailed SA is provided in the companion deliverable D3.11 aiming at identifying, classifying and analysing the main sources of uncertainties that affect the progression and consequences for the major event of Station Blackout (SBO) by relying on a SA technique termed as fast Fourier transform based methods (Prošek et al., 2002). The current overview also shows that there is no one-fits-all SA technique and depending on the characteristics of the problem, different techniques may be proposed or new developments are needed. The choice of the particular techniques is then guided by the objective of the sensitivity analysis (local, global), the type of variables as well as the problem of dependence between inputs (Table 1).

Regarding NARSIS specificities, we have identified two aspects that deserve new developments for constraining uncertainties:

(1) Since BBN is one pillar of NARSIS (see deliverable D3.2), the question of SA is specifically addressed by relying on a newly developed technique dedicated to this specific method. The most widely used approach is based on sensitivity functions for discrete BBNs, and on partial derivatives for continuous BBNs. Reasons are the intuitive interpretation of the results (thanks to the graphical presentation) and the simplicity of the implementation. Yet, these approaches only provide information on the local influence, in the sense that the parameters are varied "one-at-a-time". This means that it can only provide a restricted vision on sensitivity, because the exploration of the sensitivity remains limited to a few Conditional Probability Model (CPM) parameters, while the domain of the other CPM parameters is left mostly unexplored. In this context, the proposed Boosted Beta Regression can be considered more complete by providing global insight on the sensitivity by means of the partial effects, which directly show the individual, possibly non-linear, effects of all CPM parameters. We have shown how the BBR approach can provide richer information than existing methods at multiple levels:

- Level (1): it selects the most influential parameters and it screens those that are of negligible influence (information that is generally unknown a priori);
- Level (2): it provides the functional relation between the CPM parameters and the result of the probabilistic query. The proposed approach builds on a graphical presentation of the results, which eases the interpretation;
- Level (3): the practitioner can study how the combined effect of the CPM parameters can lead to different probabilistic regimes (e.g., situations of high probability values) by studying the evolution of the Beta mean. Furthermore, the practitioner can measure the confidence in the occurrence of the identified probabilistic regimes, by studying the effect on the Beta σ parameter.

(2) The question of components' fragility is specifically addressed by relying on the developments of an approach for uncertainty reduction in fragility assessments. These results are also useful support the developments in WP2 dedicated to fragility assessment of main NPPs critical elements. We have proposed a methodology within the Bayesian setting by combining an Artificial Neural Network, an adaptive training algorithm and an amplification-factor-based construction of the likelihood function. By application to the Kashiwazaki-Kariwa Research Initiative for Seismic Margin Assessment (KARISMA) benchmark, we have shown that the proposed tool allows to reduce epistemic uncertainties (i.e. related to the lack of knowledge also named the reducible part of uncertainty) in the fragility curves (as the ones used in NARSIS). The application of the methodology was restricted to a seismic risk analysis, but it should be underlined that the framework is flexible enough to be extended to other hazards (and associated fragility curves), in particular because of the versatility of the Bayesian setting. Second, the application takes advantage of the availability of the damage database but could easily be applied to

any inspection data coming for instance from in site monitoring exercises for instance. This could constitute a valuable basis for NARSIS WP5 for instance.

With these new developments, we believe that any practitioner of NARSIS is equipped with efficient sensitivity analysis tools to identify most influential sources of uncertainty and to set up prioritization for reducing them within the project. These developments, though dedicated to the specific aspects addressed within NARSIS, are of interest for the nuclear safety community and have been published in two journals with international audience: Rohmer and Gehl (2020) and Wang et al. (2018b).

7 References

Abdel-Khalik, H.S. (2012). Adjoint-based sensitivity analysis for multi-component models, Nuclear Engineering and Design, 245, 49- 54.

Aggarwal, C.C. (2018). An introduction to neural networks. In Neural Networks and Deep Learning; Springer, 1–52.

Bayer, F. M., Cribari-Neto, F. (2017). Model selection criteria in beta regression with varying dispersion. Communications in Statistics-Simulation and Computation, 46(1), 729-746.

Beuzen, T., Marshall, L., Splinter, K. D. (2018). A comparison of methods for discretizing continuous variables in Bayesian Networks. Environmental Modelling & Software, 108, 61-66.

Borgonovo, E., Castaings, W., Tarantola, S. (2011). Moment Independent Importance Measures: New Results and Analytical Test Cases: Moment Independent Importance Measures. Risk Analysis, 31, 404–428. https://doi.org/10.1111/j.1539-6924.2010.01519.x

Bühlmann, P., Hothorn, T. (2007). Boosting algorithms: Regularization, prediction and model fitting (with discussion). Statistical Science, 22, 477–522.

Cacuci, D.G. (2015). Second-order adjoint sensitivity analysis methodology (2nd-ASAM) for computing exactly and efficiently first- and second-order sensitivities in large-scale linear systems: I. Computational methodology. J Comput Phys., 284, 687–699.

Campolongo, F., Saltelli, A., Cariboni, J. (2011). From screening to quantitative sensitivity analysis. A unified approach. Comp. Physics Comm., 182, 978–988.

Caniou, Y. (2012). Global sensitivity analysis for nested and multiscale modelling. PhD thesis from University Blaise Pascal - Clermont II – France.

Castillo, E., Gutiérrez, J. M., Hadi, A. S. (1997). Sensitivity analysis in discrete Bayesian networks. IEEE Transactions on Systems, Man, and Cybernetics, Part A: Systems and Humans, 27(4), 412-423.

Castillo, E., Kjærulff, U. (2003). Sensitivity analysis in Gaussian Bayesian networks using a symbolic-numerical technique Reliab. Eng. Syst. Saf., 79, 139-148.

Chan, H., Darwiche, A. (2002). When do numbers really matter? J. Artif. Intell. Res., 17, 265-287.

Chan, H., Darwiche, A. (2005). A distance measure for bounding probabilistic belief change Internat. J. Approx. Reason., 38, 149-174.

Chastaing, G., Gamboa, F., Prieur, C. (2012). Generalized Hoeffding-Sobol decomposition for dependent variables - application to sensitivity analysis. Electronic Journal of Statistics, 6, 2420–2448.

Chen, S. H., & Pollino, C. A. (2012). Good practice in Bayesian network modelling. Environmental modelling & software, 37, 134–45.

Chun, M.-H., Han, S.-J., Tak, N.-I. (2000). An uncertainty importance measure using a distance metric for the change in a cumulative distribution function. Reliability Engineering & System Safety, 70, 313–321.

Cooper, G.F., (1984). NESTOR: a Computer-based Medical Diagnostic Aid that Integrates Causal and Probabilistic Knowledge. Report HPP-84-48, Stanford University.

Coupé, V. M. H., & van der Gaag, L. C. (2002). Properties of sensitivity analysis of Bayesian belief networks. Ann. Math. Artif. Intell., 36, 323-356.

Cribari-Neto, F., Zeileis, A. (2010). Beta regression in R. Journal of Statistical Software, 34.

Da Veiga, S., Wahl, F., Gamboa, F. (2009). Local Polynomial Estimation for Sensitivity Analysis on Models With Correlated Inputs. Technometrics, 51, 452–463.

de Crecy, A., Bazin, P., Glaeser, H., Skorek, T., Joucla, J., Probst, P., Fujioka, K., Chung, B.D., Oh, D.Y., Kyncl, M., Pernica, R., Macek, J., Meca, R., Macian, R., D'Auria, F., Petruzzi, A., Batet, L., Perez, M., Reventos, F. (2008). Uncertainty and sensitivity analysis of the LOFT L2-5 test: Results of the BEMUSE programme. Nucl. Eng. Des., 238, 3561–3578.

Der Kiureghian, A., Ditlevsen, O. (2009). Aleatory or epistemic? Does it matter?. Structural safety, 31(2), 105-112.

de Rocquigny E., Devictor N., Tarantola S. (editors) (2008). Uncertainty in industrial practice, A guide to quantitative uncertainty management, Wiley, 364 p.

Doksum, K. A. G. L. Sievers, (1976). Plotting with confidence: graphical comparisons of two populations. Biometrika, 63(3), 421–434.

Druzdzel, M.J., van der Gaag, L. (2000). Building Probabilistic Networks: “where do the numbers come from?” IEEE Trans. Knowl. Data Eng., 12(4), 481–486.

Eilers, P. H. C., Marx, B. D. (1996). Flexible smoothing with B-splines and penalties. Statistical Science, 11, 89–121.

EPRI (2014), Assessment of the Use of Experience Data to Develop Seismic Fragilities, Research Report 3002002933, Palo Alto.

EPRI (2009), Seismic fragility application guide. Technical Report TR-1019200 Palo Alto.

Espinheira, P. L., Ferrari, S. L. P., Cribari-Neto, F., (2008). On beta regression residuals. Journal of Applied Statistics, 35 (4), 407-419.

Fang, S., Gertner, G.Z., Anderson, A.A. (2004). Estimation of sensitivity coefficients of nonlinear model input parameters which have a multinormal distribution. Computer Physics Communications, 157, 9–16. https://doi.org/10.1016/S0010-4655(03)00488-0

Ferrari, S., Cribari-Neto, F. (2004). Beta regression for modelling rates and proportions. Journal of Applied Statistics, 31(7), 799-815.

Frepoli, C., Petruzzi, A. (2008). Scaling, Uncertainty, and 3D Coupled Code Calculations in Nuclear Technology. Science and Technology of Nuclear Installations, 7-9.

van Der Gaag, L. C., Kuijper, R., Van Geffen, Y. M. & Vermeulen, J. L. (2013). Towards uncertainty analysis of Bayesian Networks. In 25th Benelux Conference on Artificial Intelligence, Delft, The Netherlands.

Gehl, P., Marcilhac-Fradin, M., Rohmer, J., Guigueno, Y., Rahni, N., and Clément, J. (2019). Identifying Uncertainty Contributions to the Seismic Fragility Assessment of a Nuclear Reactor Steam Line, in: 7th International Conference on Computational Methods in Structural Dynamics and Earthquake Engineering, Crete, Greece.

Gehl, P., Rohmer, J. (2018). Vector intensity measures for a more accurate reliability assessment of NPP sub-systems. In International Conference on Technological Innovations in Nuclear Civil Engineering, Saclay, France.

Gehl, P., D’Ayala, D. (2016). Development of Bayesian Networks for the multi-hazard fragility assessment of bridge systems. Structural Safety, 60, 37-46.

Glaeser, H. (2008). GRS Method for Uncertainty and Sensitivity Evaluation of Code Results and Applications., Science and Technology of Nuclear Installations, 112-118.

Gómez-Villegas, M.A., Main, P., Susi, R. (2007). Sensitivity analysis in Gaussian Bayesian networks using a divergence measure. Comm. Statist. Theory Methods, 36(3), 523-539.

Gómez-Villegas, M. A., Main, P., Susi, R. (2013). The effect of block parameter perturbations in Gaussian Bayesian networks: sensitivity and robustness. Inform. Sci., 222, 439-458.

Grandjacques, M., Delinchant, B., Adrot, O. (2015). Pick and freeze estimation of sensitivity index for static and dynamic models with dependent inputs. Retrieved from https://hal.archives-ouvertes.fr

Grün, B., Kosmidis, I., Zeileis, A. (2012). Extended Beta Regression in R: Shaken, Stirred, Mixed, and Partitioned. Journal of Statistical Software, 48(11), 1–25.

Hänninen, M., Banda, O. A. V., Kujala, P. (2014). Bayesian network model of maritime safety management. Expert Systems with Applications, 41(17), 7837-7846.

Hastings, W. K. (1970). Monte Carlo sampling methods using Markov chains and their applications. Biometrika, 57(1), 97-109.

Heckerman, D., Horwitz, E. Nathwani, B. (1992). Towards Normative Expert Systems: Part I. The Pathfinder Project. Methods of Information in Medicine, 31, 90-105.

Hernández-Solís, A. (2012). Uncertainty and sensitivity analysis applied to LWR neutronic and thermal-hydraulic calculations, PhD Thesis Chalmers University of Technology, Sweden.

Heinze-Deml, C., Maathuis, M. H., Meinshausen, N. (2018). Causal structure learning. Annual Review of Statistics and Its Application, 5, 371-391.

Hofner, B., Mayr, A., Schmid, M. (2016). gamboostLSS: An R package for model building and variable selection in the GAMLSS framework. Journal of Statistical Software, 74(1).

Homma, T., Saltelli, A. (1996). Importance measures in global sensitivity analysis of nonlinear models. Reliability Engineering and System Safety, 52,1-17.

Humbird, K.D., McClarren, R.G. (2017). Adjoint-based sensitivity analysis for high-energy density radiative transfer using flux-limited diffusion. High Energy Density Phys., 22, 12-16.

Iman, R.L., Hora, S.C. (1990). A Robust Measure of Uncertainty Importance for Use in Fault Tree System Analysis. Risk Analysis, 10, 401–406. https://doi.org/10.1111/j.1539-6924.1990.tb00523.x

International Atomic Energy Agency IAEA (2008). Best Estimate Safety Analysis for Nuclear Power Plants: Uncertainty Evaluation. Safety Reports Series No. 52, IAEA, Vienna (2008).

International Atomic Energy Agency IAEA (2014). Review of Seismic Evaluation Methodologies for Nuclear Power Plants Based on a Benchmark Exercise. IAEA-TECDOC-1722, IAEA, Vienna (2014).

Iooss, B., Lemaître, P. (2015). A review on global sensitivity analysis methods. In Uncertainty management in simulation-optimization of complex systems (pp. 101-122). Springer, Boston, MA.

Iooss, B., Prieur, C. (2019). Shapley effects for sensitivity analysis with dependent inputs: comparisons with Sobol' indices, numerical estimation and applications. International Journal for Uncertainty Quantification, 9(5).

Jackson, P. (1999). Introduction to expert systems, third edition, Addison-Wesley.

Jacques, J., Lavergne, C., Devictor, N. (2006). Sensitivity analysis in presence of model uncertainty and correlated inputs. Reliability Engineering & System Safety, 91, 1126–1134. https://doi.org/10.1016/j.ress.2005.11.047

Jäger, W. S., Christie, E. K., Hanea, A. M., den Heijer, C., Spencer, T. (2018). A Bayesian network approach for coastal risk analysis and decision making. Coastal Engineering, 134, 48-61.

Jaeger, W., Sanchez Espinoza, V., Mayorga, F. J. M., Queral, C. (2017). Uncertainty and Sensitivity Investigations with TRACE-SUSA and TRACE-DAKOTA by Means of Post-test Calculations of NUPEC BFBT Experiments, NUREG/IA-0462.

Jensen, F.B. (2001). Networks and Decision Graphs. Springer, New York.

Jones, P.J., Mair, P., Simon, T., Zeileis, A. (2019). Network Model Trees, OSF ha4cw, OSF Preprints. doi:10.31219/osf.io/ha4cw

Kleemann, J., Celio, E., Fürst, C., (2017). Validation approaches of an expert-based Bayesian Belief Network in Northern Ghana, West Africa. Ecol. Model., 365, 10–29.

Koenker, R., Leorato, S., Peracchi, F. (2013). Distributional vs. Quantile Regression. Technical Report 300, Centre for Economic and International Studies, University of Rome Tor Vergata, Rome, Italy.

Koller, D., Friedman, N. (2009). Probabilistic Graphical Models: Principles and Techniques. MIT Press.

Kucherenko, S., Tarantola, S., Annoni, P. (2012). Estimation of global sensitivity indices for models with dependent variables. Computer Physics Communications, 183, 937–946. https://doi.org/10.1016/j.cpc.2011.12.020

Kwag, S., Gupta, A. (2017). Probabilistic risk assessment framework for structural systems under multiple hazards using Bayesian statistics. Nuclear Engineering and Design, 315, 20-34.

Laskey, K. B. (1995). Sensitivity analysis for probability assessments in Bayesian networks IEEE Trans. Syst. Man Cybern., 25(6), 901-909.

Lemke, M., Cai, L., Reiss, J., Pitsch, H., Sesterhenn, J. (2019). Adjoint-based sensitivity analysis of quantities of interest of complex combustion models, Combustion Theory and Modelling, 23(1), 180-196.

Leonelli, M., Goergen, C., Smith, J. Q. (2017). Sensitivity analysis in multilinear probabilistic models. Information Sciences, 411, 84–97.

Li, C., Mahadevan, S. (2016). An efficient modularized sample-based method to estimate the first-order Sobol index. Reliability Engineering & System Safety, 153, 110–121. https://doi.org/10.1016/j.ress.2016.04.012

Li, G., Rabitz, H., Yelvington, P.E., Oluwole, O.O., Bacon, F., Kolb, C.E., Schoendorf, J. (2010). Global Sensitivity Analysis for Systems with Independent and/or Correlated Inputs. The Journal of Physical Chemistry A, 114, 6022–6032. https://doi.org/10.1021/jp9096919

Li, L., Lu, Z., Zhou, C. (2011). Importance analysis for models with correlated input variables by the state dependent parameters method. Computers & Mathematics with Applications, 62, 4547–4556. https://doi.org/10.1016/j.camwa.2011.10.034

López-Benito, A., Bolado-Lavín, R. (2017). A case study on global sensitivity analysis with dependent inputs: The natural gas transmission model. Reliability Engineering & System Safety, 165, 11–21.

Malagrino, L. S., Roman, N. T., & Monteiro, A. M. (2018). Forecasting stock market index daily direction: a Bayesian network approach. Expert Systems with Applications, 105, 11-22.

Mara, T.A., Tarantola, S. (2012). Variance-based sensitivity indices for models with dependent inputs. Reliability Engineering & System Safety, 107, 115–121.

Marcot, B. G., & Penman, T. D., (2019). Advances in Bayesian network modelling: Integration of modelling technologies. Environmental modelling & software, 111, 386-393.

Mayr, A., Fenske, N., Hofner, B., Kneib, T., Schmid, M. (2012). Generalized additive models for location, scale and shape for high dimensional data - a flexible approach based on boosting. Journal of the Royal Statistical Society, Series C, 61, 403–427.

McClarren R. G. (2018). Uncertainty Quantication and Predictive Computational Science. A Foundation for Physical Scientists and Engineers. Springer Nature Switzerland.

McKay, M.D. (1995). Evaluating prediction uncertainty. Nuclear Regulatory Commission. NUREG/CR—6311.

Meinshausen, N., Bühlmann, P. (2010). Stability selection. Journal of the Royal Statistical Society: Series B (Statistical Methodology), 72(4), 417-473.

Milns, I., Beale, C. M., & Smith, V. A. (2010). Revealing ecological networks using Bayesian network inference algorithms. Ecology, 91(7), 1892-1899.

Murphy, K. P. (1999). A variational approximation for Bayesian networks with discrete and continuous latent variables. In 15th conference on Uncertainty in artificial intelligence. Morgan Kaufmann Publishers Inc.

Oakley, J.E., O'Hagan, A. (2004). Probabilistic sensitivity analysis of complex models: a Bayesian approach. Journal of the Royal Statistical Society: Series B (Statistical Methodology), 66, 751–769.

Pan, F., Zhu, J., Ye, M., Pachepsky, Y.A., Wu, Y.-S. (2011). Sensitivity analysis of unsaturated flow and contaminant transport with correlated parameters. Journal of Hydrology, 397, 238–249.

Parkinson, W., Rasmussen, N., Hinkle, W. (1979). Sensitivity analysis of the reactor safety study, MIT EL79-008, MIT NE-225.

Pereira, G. H. (2019). On quantile residuals in beta regression. Communications in Statistics-Simulation and Computation, 48(1), 302-316.

Perez, M., Reventos, F., Batet, L., Guba, A., Toth, I., Mieusset, T., Bazin, P., de Crecy, A., Borisov, S., Skorek, T., Glaeser, H., Joucla, J., Probst, P., Ui, A., Chung, B.D., Oh, D.Y., Pernica, R., Kyncl, M., Macek, J., Manera, A., Freixa, J., Petruzzi, A., D'Auria, F., Del Nevo, A. (2011). Uncertainty and sensitivity analysis of a LBLOCA in a PWR Nuclear Power Plant: Results of the Phase V of the BEMUSE programme. Nucl. Eng. Des., 241, 4206–4222.

Petruzzi, A., D'Auria, F., (2008). Approaches, Relevant Topics, and Internal Method for Uncertainty Evaluation in Predictions of Thermal-Hydraulic System Codes. Science and Technology of Nuclear Installations, 17-33.

Pheulpin, L. (2020). Methodologies on uncertainty quantification and global sensitivity analysis with dependent inputs: Review and application to a simplified case of inundation (No. IRSN/2020-00321). IRSN/PSE-ENV/SCAN/BEHRIG.

Pheulpin, L., Bacchi, V., (2020). Uncertainty quantification and global sensitivity analysis with dependent inputs: Application to the 2D hydraulic model of the Loire River. Presented at the EGU 2020-18939.

Pitchforth, J., Mengersen, K. (2013). A proposed validation framework for expert elicited Bayesian Networks. Expert Systems with Applications, 40(1), 162-167.

Prošek, A. Leskovar, M. (2015), Use of FFTBM by signal mirroring for sensitivity study. Annals of Nuclear Energy, 76: 253-262.

Prošek, A. Mavko, B. (2007). The state-of-the-art theory and applications of best-estimate plus uncertainty methods, Nuclear tTechnology, 158, 69-79.

Prošek, A., D'Auria, F., Mavko, B. (2002). Review of quantitative accuracy assessments with fast Fourier transform based methods (FFTBM). Nuclear Engineering and Design, 217, 179-206.

Puy, A., Lo Piano, S., Saltelli, A. (2020). Is VARS more intuitive and efficient than Sobol' indices, arXiv:2009.12558.

Qiu, Y., Aufiero, M., Wang, K., Fratoni, M. (2016). Development of sensitivity analysis capabilities of generalized responses to nuclear data in Monte Carlo code RMC, Annals of Nuclear Energy, 97, 142-152.

Radulescu, G., Mueller, D.E., Wagner J.C., (2008). Sensitivity and Uncertainty Analysis of Commercial Reactor Criticals for Burnup Credit, US NRC Y6517.

Ratto, M., Tarantola, S., Saltelli, A., Young, P.C. (2004). Accelerated estimation of sensitivity indices using state dependent parameter models In Proc. Conf. on Sensitivity Analysis of Model Output (SAMO) (pp. 8-11).

Rearden, B. T. (2000). Sensitivity and Uncertainty Analysis for Nuclear Criticality Safety Using KENO in the SCALE Code System, Computational Physics and Engineering Division (10).

Rigby, R. A., Stasinopoulos, D. M. (2005). Generalized additive models for location, scale and shape. Journal of the Royal Statistical Society: Series C (Applied Statistics), 54(3), 507-554.

Rohmer, J., Gehl, P. (2020). Sensitivity analysis of Bayesian networks to parameters of the conditional probability model using a Beta regression approach. Expert Systems with Applications, 145, 113130.

Ronen, Y. (1986). Handbook of Nuclear Reactors Calculations, Volume III, CRC Press, United States.

Russell, S., Norvig, P., Canny, J., Malik, J., Edwards, D. (2003). Artificial intelligence: a modern approach. Prentice Hall, Englewood Cliffs.

Saltelli, A., Aleksankina, K., Becker, W., Fennell, P., Ferretti, F., Holst, N., Li, S., Wu, Q. (2019). Why so many published sensitivity analyses are false: A systematic review of sensitivity analysis practices. Environmental modelling & software, 114, 29-39.

Saltelli, A., Tarantola, S., Campolongo, F., & Ratto, M. (2004). Sensitivity analysis in practice: a guide to assessing scientific models (Vol. 1). New York: Wiley.

Schmid, M., Wickler, F., Maloney, K. O., Mitchell, R., Fenske, N., Mayr, A. (2013). Boosted beta regression. PloS one, 8(4), e61623.

Skorek, T., de Crécy, A., et al. (2019). Quantification of the uncertainty of the physical models in the system thermal-hydraulic codes–PREMIUM benchmark. Nuclear Engineering and Design, 354, 110199.

Smithson, M., Verkuilen, J. (2006). A better lemon squeezer? Maximum-likelihood regression with beta-distributed dependent variables. Psychological Methods, 11, 54–71.

Smyth, G., Verbyla, A. (1999). Adjusted likelihood methods for modelling dispersion in generalized linear models. Environmetrics, 10(6), 695–709.

Scutari, M., Howell, P., Balding, D. J., Mackay, I. (2014). Multiple quantitative trait analysis using Bayesian networks. Genetics, 198(1), 129-137.

Shenoy, P.P. (2006). Inference in hybrid Bayesian networks using mixtures of Gaussians Uncertainty in artificial intelligence, AUAI Press, Corvallis, 428-436.

Sobol, I.M. (2001). Global sensitivity indices for nonlinear mathematical models and their Monte Carlo estimates, Math. and Comp. in Simulation, 55, 271–280.

Soto, O., Löhner, R., Yang, C. (2004). An adjoint-based design methodology for CFD problems, Int. Jour. of Numerical Methods for Heat and Fluid Flow, 734-759.

Straub, D., Der Kiureghian, A. (2008). Improved seismic fragility modeling from empirical data. Structural safety, 30(4), 320-336.

Strydom, G., Bostelmann, F. (2017). Nuclear data uncertainty and sensitivity analysis of the VHTRC benchmark using SCALE, INL/JOU-17-42606-Revision-0.

Renooij, S. (2014). Co-variation for sensitivity analysis in Bayesian networks: Properties, consequences and alternatives. International Journal of Approximate Reasoning, 55(4), 1022-1042.

Ţene, M., Stuparu, D.E., Kurowicka, D., El Serafy, G.Y., 2018. A copula-based sensitivity analysis method and its application to a North Sea sediment transport model. Environmental Modelling & Software, 104, 1–12.

Thomas, J., Mayr, A., Bischl, B., Schmid, M., Smith, A., and Hofner, B. (2018), Gradient boosting for distributional regression - faster tuning and improved variable selection via noncyclical updates. Statistics and Computing, 28, 673-687.

Umminger, K., Del Nevo A. (2012). Integral Test Facilities and Thermal-Hydraulic System Codes in Nuclear Safety Analysis. Science and Technology of Nuclear Installations, 7-10.

Wang, Z., Pedroni, N., Zentner, I., and Zio, E. (2018a). Seismic fragility analysis with artificial neural networks: Application to nuclear power plant equipment. Eng. Struct.,162, 213–225.

Wang, Z., Zentner, I., Zio, E. (2018b) A Bayesian framework for estimating fragility curves based on seismic damage data and numerical simulations by adaptive neural networks. Nuclear Engineering and Design, 338, 232-246.

Wang, P., Lu, Z., Zhang, K., Xiao, S., Yue, Z. (2018c). Copula-based decomposition approach for the derivative-based sensitivity of variance contributions with dependent variables. Reliability Engineering & System Safety, 169, 437–450. https://doi.org/10.1016/j.ress.2017.09.012

Weber, P., Medina-Oliva, G., Simon, C., & Iung, B. (2012). Overview on Bayesian networks applications for dependability, risk analysis and maintenance areas. Engineering Applications of Artificial Intelligence, 25(4), 671-682.

Wiegerinck, W., Kappen, B., Burgers, W. (2010). Bayesian networks for expert systems: Theory and practical applications. In Interactive collaborative information systems. Springer, Berlin, Heidelberg, 547-578.

Xu, C., Gertner, G.Z. (2008). Uncertainty and sensitivity analysis for models with correlated parameters. Reliability Engineering & System Safety, 93, 1563–1573.

Young, J., Graham, P., Penny, R. (2009). Using Bayesian networks to create synthetic data. Journal of Official Statistics, 25(4), 549-567.

Zhao H., Mousseau V.A. (2012). Use of forward sensitivity analysis method to improve code scaling, applicability, and uncertainty (CSAU) methodology. Nuclear Engineering and Design, 249, 188-196.

Zhou, C., Lu, Z., Li, L., Feng, J., Wang, B. (2013). A new algorithm for variance based importance analysis of models with correlated inputs. Applied Mathematical Modelling 37, 864–875.

8 Appendix A

The analysis of Bayesian Belief Network relies on conditional probabilities. Consider $X_{i=1,\dots,n}$ the *n* nodes of the BBN. The joint probability distribution can be expressed using conditional probability as:

$$P(X_1, X_2, \dots, X_n) = \prod_{i=1}^{n} P(X_i | X_1, \dots, X_{i-1}) \quad \text{(Eq. A1)}$$

This equation simplifies under the conditional independence assumption as:

$$P(X_1, X_2, \dots, X_n) = \prod_{i=1}^{n} P(X_i | \mathrm{Pa}(X_i)) \quad \text{(Eq. A2)}$$

where $\mathrm{Pa}(X_i)$ corresponds to the parent nodes of X_i. For discrete nodes, the value of $P(X_i|\mathrm{Pa}(X_i))$ is the entry of the Conditional Probability Table. For continuous nodes, $P(X_i|\mathrm{Pa}(X_i))$ can be modelled by a continuous probability distribution whose parameters depend on the values of the parent nodes.

Conditional queries aim at evaluating the conditional probability of some event, e.g. node X_j takes up the value *x* when new information/observations become available, i.e. given new "evidence" (denoted *e*), namely $P(X_j=x \mid e)$. This procedure, termed as query, relies on inference techniques. Exact inference in a BBN is possible, but is generally not possible in large networks. For networks, which contain a large number of nodes, arcs, or have nodes comprised of variables with large numbers of levels, exact inference becomes too computationally intensive. Among the possible approximate inference algorithms, the present study relies on the logic sampling method (Koller and Friedman 2009), which works from the root nodes down to the leaf nodes. First, a random draw from each of the leaf nodes is taken with probabilities equal to the respective levels. The distributions for the next level of nodes can then be marginalized based on the draws obtained from their parents. From these marginal distributions a random draw is again taken respective of the categorical probabilities. This process is repeated until a draw has been taken from every node in the network. This completed case represents a single sample. After many samples have been taken, the samples are subsetted to the cases which match the evidence of interest. Estimated probabilities can then be obtained for any node of interest from this subset of the samples.

9 Appendix B

We first describe the principles of model-based gradient boosting (Sect. B1), and describe how to apply it within the GAMLSS framework (Sect. B2).

B1 Gradient boosting

This supervised learning technique (e.g., Bühlmann and Hothorn, 2007) combines an ensemble of simple regression models (termed as base-learners), such as linear regression models or regression splines of low degree of freedom, to estimate complex functional relationships.

Consider the training dataset $\boldsymbol{D}=\{\boldsymbol{C}^{(j)}, P^{(j)}\}_{j=1,\ldots,n}$ where $\boldsymbol{C}$ is the vector of p predictor variables $c_{i=1,\ldots,p}$ and P is the variable of interest, whose expected value (possibly its transformed value) is modelled by an additive model as follows:

$$\eta(\boldsymbol{C}) = \beta_0 + \sum_{j=1}^{J} f_j(c_j|\beta_j) \qquad \text{(Eq. B1)}$$

where $J \leq p$, β_0 is a constant intercept and the additive effects $f_j(c_j|\beta_j)$ are pre-defined univariate base-learners, which typically correspond to (semi-)parametric effects with parameter vector β_j.
To estimate the parameters β_j, the boosting algorithm minimizes the empirical risk R, which corresponds to the sum of loss function ρ over all training data:

$$R = \sum_{j=1}^{n} \rho(P^{(j)}, \eta(\boldsymbol{C}^{(j)})) \qquad \text{(Eq. B2)}$$

where the loss function ρ can take different forms, such as the quadratic loss $(P^{(j)} - \eta(\boldsymbol{C}^{(j)}))^2$, which corresponds to the ordinary least square regression or more generally, it can correspond to the negative log-likelihood of the distribution of the variable of interest P (in the case considered here, this corresponds to the Beta distribution).

Among the different boosting algorithms, we focus on the component-wise gradient boosting approach of Bühlmann and Hothorn (2007). Instead of focusing on the true outcomes $\boldsymbol{P}=(P^{(1)}, P^{(2)},\ldots, P^{(n)})$, this procedure aims at fitting simple regression-type base learners $h(.)$ one by one to the negative gradient vector of loss $\boldsymbol{u}=(u^{(1)}, u^{(2)},\ldots, u^{(n)})$. The objective is to approximate the jth effect $f_j(c_j|\beta_j) = \sum_m h_j(.)$ at iteration m of the algorithm. Formally, $\boldsymbol{u}$ is evaluated considering the current estimated (i.e. iteration m-1) additive predictor model $\hat{\eta}^{[m-1]}(\boldsymbol{C}^{(j)})$ as follows:

$$\boldsymbol{u} = \left(-\frac{\partial}{\partial \eta} \rho(P, \eta)_{|_{\eta=\hat{\eta}^{[m-1]}(\boldsymbol{C}^{(j)}), P=P^{(j)}}} \right)_{j=1,\ldots,n} \qquad \text{(Eq. B3)}$$

In every boosting iteration, each base-learner is fitted separately to the negative gradient vector. The best-fitting base-learner is then selected based on the residual sum of squares with respect to $\boldsymbol{u}$ as follows:

$$j^* = \underset{j \in 1,\ldots,J}{\operatorname{argmin}} \sum_{i=1}^{n} (u^{(i)} - h_j(\boldsymbol{C}^{(i)}))^2 \qquad \text{(Eq. B4)}$$

The selected base-leaner is used to update the current predictor model as follows:

$$\hat{\eta}^{[m]} = \hat{\eta}^{[m-1]} + s.h_{j*}(\boldsymbol{C}) \qquad \text{(Eq. B5)}$$

where s is a step length (with typical value of 0.1).

The main tuning parameter is the number of iterations m, which directly determines the prediction performance. If m is too large, rich models with large number of predictors and rough functional terms will be constructed (hence leading to overfitting), which might hamper the interpretability of the resulting model. If m is too low, sparse models with smooth functional terms will be constructed but with the danger of missing some important predictor variables. In practice, the selection of m can be carried out using cross-validation procedures in order to optimize the predictive risk on observations left out from the fitting process i.e. the "out-of-bag" risk which corresponds to the negative log-likelihood for the considered probabilistic distribution calculated for the "out-of-bag" samples.

B2 Boosted GAMLSS

The afore-described algorithm can be applied to the GAMLSS framework by cycling through the distribution parameters θ in the fitting process (Thomas et al., 2018: Algorithm 1). In each iteration, the best fitting base-learner is evaluated for each distribution parameter, while the other ones remain fixed. For a probability distribution with two parameters (like the Beta distribution), the update in the boosting algorithm at iteration *m* holds as follows:

$$\frac{\partial}{\partial \eta_{\theta_1}} \rho\left(P, \theta_1^{[m]}, \theta_2^{[m]}\right) \xrightarrow{\text{update}} \eta_{\theta_1}^{[m+1]} \quad \text{(Eq. B6)}$$

$$\frac{\partial}{\partial \eta_{\theta_2}} \rho(P, \theta_1^{[m]}, \theta_2^{[m]}) \xrightarrow{\text{update}} \eta_{\theta_2}^{[m+1]} \quad \text{(Eq. B7)}$$

In the original cyclic algorithm, (see algorithm 1 described by Thomas et al. (2018)), separate stopping values have to be specified for each parameter, which motivated the development of a noncyclic algorithm (algorithm 2 by Thomas et al. (2018)), which avoids optimizing two different stopping iterations and reducing the optimisation problem from a multi-dimensional to a one-dimensional problem.

10 Appendix C

This appendix describes the procedure for stability selection (Meinhausen and Bühlmann, 2010). Consider p predictor variables $c_{j=1,\ldots,p}$ and the predictand *P*. Based on n observations, the stability selection with boosting proceeds as follows:

Step 1. Select a random subset of size [n/2] of the data (where [n/2] corresponds to the largest integer $\leq$ n/2);

Step 2. Fit a boosting model and continue to increase the number of boosting iteration until *q* base-learners are selected. $\hat{S}_{\lfloor \frac{n}{2} \rfloor}$ corresponds to the set of selected variables;

Step 3. Repeat steps 1 and 2 for *b*=1,…,*B*;

Step 4. Compute the selection probabilities per base learner as follows:

$$P_j = \frac{1}{B}\sum_{b=1}^{B} \mathbf{I}_{\{j \in \hat{S}_{\lfloor \frac{n}{2} \rfloor, b}\}} \quad \text{(Eq. C1)}$$

where **I**(A) is the indicator function, which reaches 1 if A is true, 0 otherwise.

Step 5. Select all base-learners associated to a selection probability of at least *t*. The set of stable selected variables is thus $\hat{S} = \{j: P_j \geq t\}$.

Meinhausen and Bühlmann (2010) studied the error of selecting false positive variables (i.e. noise variables) and showed that the selection procedure controls the per-family error rate (*PFER*) and an upper bound is provided as follows:

$$PFER \leq \frac{q^2}{(2t-1)p} \quad \text{(Eq. C2)}$$

where *q* is the number of selected variables per boosting iteration, *p* is the number of (possible) predictors and *t* is the selection threshold. In practice, at least two of these parameters have to be specified to run the procedure. In the application case of Sect. 4.4, we specified the upper bound of *PFER* (set up at 1) and *q* at 10. An extensive investigation of the applicability of this procedure for distributional regression within the boosted GAMLSS setting has been carried out by Thomas et al. (2018).

11 Appendix D

The following appendix describes the main formulations of the residuals for Beta regression based on Pereira (2019) and references therein.

Let us consider the raw response residuals for the i[th] observation P_i defined as $r_i = P_i - \widehat{P}_i$ where $\hat{P}$ is the mean μ predicted by BBR model (see Sect. 4.2 for the description of the parameters). For sake of presentation, let us consider the Beta parameter $\varphi = \frac{1}{\sigma^2} - 1$ where σ is defined in Sect. 2.1.

The deviance residual is defined as:

$$r_i^{deviance} = r_i.\sqrt{2|L(P,\varphi) - L(\mu,\varphi)|} \quad \text{(Eq. D1)}$$

where the bivariate function $L(.,.)$ holds as follows:

$$L(\mu,\varphi) = lI\Gamma(\varphi) - lI\Gamma(\varphi.\mu) - lI\Gamma\big((1-\mu).\varphi\big) + (\mu.\varphi - 1).\log(P) + \big((1-\mu).\varphi - 1\big).\log(1-P) \quad \text{(Eq. D2)}$$

where $lI\Gamma(.)$ is natural logarithm of the absolute value of the gamma function.

The 'standardized weighted residual 1' originally introduced by Espinheira et al. (2008) is defined as follows:

$$r_i^{weighted} = \frac{P^* - \mu^*}{\sqrt{v}} \quad \text{(Eq. D3)}$$

where P^* is the quantile for the logistic distribution with location set up at zero and scale at one, and

$$\mu^* = \Gamma''(\mu.\varphi) - \Gamma''((1-\mu).\varphi) \quad \text{(Eq. D4)}$$

$$v = \Gamma'''(\mu.\varphi) - \Gamma'''((1-\mu).\varphi) \quad \text{(Eq. D5)}$$

where Γ'' and Γ''' are respectively the second and third derivative of the Γ function.

The quantile residual is defined as:

$$r_i^{Quantile} = \Phi^{-1}(F(P,\mu,\varphi)) \quad \text{(Eq. D6)}$$

where Φ^{-1} is the inverse of the cumulative probability function of the standard normal distribution and F is the cumulative probability function of the Beta law.